Running Head: SEQUENCE STRATIGRAPHY OF TEXAS MIDDLE PERMIAN PLATFORM CARBONATES

OUTCROP-BASED CHARACTERiZATION OF LEONARDIAN PLATFORM CARBONATE IN WEST TEXAS: IMPLICATIONS FOR SEQUENCE STRATIGRAPHIC STYLES IN TRANSITIONAL ICEHOUSE-GREENHOUSE SETTINGS

Stephen C. Ruppel, W. Bruce Ward[1], and Eduardo E. Ariza

Bureau of Economic Geology

The University of Texas at Austin

[1] Current address: Earthworks LLC, P.O. Box 178, Newtown, CT 06470-0178

ABSTRACT

The Sierra Diablo Mountains of West Texas contain world class exposures of lower and middle Permian platform carbonates. As such these outcrops offer key insights into the products of carbonate deposition in the transitional icehouse/greenhouse setting of the early-mid Permian that are available in few other places in the world. They also afford an excellent basis for examing how styles of facies and sequence development vary between platform tops and platform margins. Using outcrop data and observations from over 2 mi (3 km) of continuous exposure, we collected detailed data on the facies composition and architecture of high frequency (cycle-scale) and intermediate frequency (high frequency sequence scale) successions within the Leonardian. We used these data to define facies stacking patterns along depositional dip across the platform in both low and high accommodation settings and to document how these patterns vary systematically between and within sequences . These data not only provide a basis for interpreting similar Leonardian platform successions from less well constrained outcrop and subsurface data sets but also point out some important caveats that should be considered serve as an important model for understanding depositional processes during the is part of the Permian worldwide.

INTRODUCTION

The Leonardian Stage (Kungurian, latest Cisuralian) was a time of marked global change in terms of climate and eustasy (Veevers and Powell, 1987; Read, 1995; Montanez and others, 2007). In the south-central U.S. it was a period marked by declining tectonic activity and changing geographies owing to the final assembly of

Pangaea. Globally the high-amplitude eustatic variations generated by marked fluctuations in polar ice volume of the late Carboniferous were giving way to more uniform climatic and sea-volume conditions of the later Paleozoic and Mesozoic. Leonardian rocks document depositional styles transitional between those of the late Carboniferous icehouse and later Permian greenhouse. Not surprisingly, these rocks display both similarities to and marked differences from both.

Despite their uniqueness and abundance, few in-depth studies of upper Cisuralian deposits have been published. Detailed studies of younger Permian successions have been published, however (e.g., Tucker, 1991; Kerans and Fitchen, 1995; Strohmenger and Strauss, 1996, Strohmenger and others, 1996—Zechstein Basin, North Sea region; Sharland and others, 2001; Stemmerik, 2001—Guadalupian, Sverdrup Basin, Greenland; Kerans and Kempter, 2002—Guadalupian, Permian Basin, Texas; Angiolini and others, 2003—Khuff Formation, Oman; Mertmann, 2003—Guadalupian, Lopingian, Pakistan), and these provide important insights into the sequence stratigraphy and facies character of older, Kungurian rocks.

This paper describes styles of facies stacking and cycle development in Leonardian rocks from continuous outcrops in the Permian Basin of West Texas. These deposits provide important insights into styles of facies accumulation and cycle development in transitional icehouse-greenhouse carbonate and offer important lessons about the application of sequence stratigraphic methods in such settings.

LOCAL SETTING

Leonardian Series rocks in the Permian Basin of West Texas and New Mexico were deposited on a well-developed array of shallow-water carbonate platforms and

deep-water basins (Figure 1). Platform successions consist of thick (up to 2,500 ft [800 m]) intervals of dominantly shallow-water peritidal and subtidal facies. Slope and basinal rocks are dominated by deep-water deposits of sandstone turbidites and carbonate debris flows of similar thicknesses. Excellent outcrops of Leonardian platform, slope, and basinal deposits are exposed in mountains in West Texas and New Mexico, especially in the Guadalupe, Brokeoff, and Sierra Diablo ranges along the west margin of the Permian Basin (Figure 1).

In the subsurface of the Permian Basin, Leonardian rocks are charged with hydrocarbons. Estimates indicate that Leonardian reservoirs contained more than 14.5 billion barrels of oil at discovery, or 15 percent of the total resource in the Permian Basin (Tyler and Banta, 1989). Because of extensive drilling for oil and gas in the basin over the years, considerable volumes of geophysical and core data are available for these rocks. Studies of subsurface data sets (primarily at the oil-field scale) have provided good insights into basic aspects of depositional and diagenetic processes and products. The 1-dimensionality of well data (wireline logs and cores) and the limited resolution of 2- and 3-dimensional data (seismic surveys), however, preclude development of accurate models of facies distribution or stratigraphic architecture. By contrast, the large-scale outcrops in West Texas and southeastern New Mexico provide 1-, 2-, and 3-dimensional displays of Leonard facies, diagenesis, and sequence stratigraphic relationships that form a fundamental basis for improving interpretation of subsurface data sets.

Herein we report on the results of fine-scale investigations of a significant part of the Leonardian shallow-water platform succession in continuously exposed outcrops in the Sierra Diablo of West Texas (Figure 2). The purpose of this research was to

improve concepts and models of Leonardian platform-carbonate development and better explain sequence stratigraphic styles. Findings of the study offer new insights into styles of facies development and sequence- and cycle-stratigraphic architecture in Leonardian carbonate-platform successions and provide models for better interpretation and understanding of the Leonard in the subsurface of the Permian Basin and of similar middle Permian successions.

AREA OF STUDY

Most outcrops of Leonardian carbonate-platform successions in the Texas and New Mexico area are poorly exposed or inaccessible. Striking exceptions are outcrops in the Sierra Diablo in Hudspeth and Culberson Counties, Texas. Here, the Leonard is exceedingly well exposed (Figure 3) and accessible in the area of Apache Canyon on the Figure 2 and Puett Ranches (Figure 2). The Sierra Diablo Mountains are situated on the west edge of the Delaware Basin of the greater Permian Basin. Leonardian outcrops in the Sierra Diablo range consist of about 1,200 ft (360 m) of platform facies and 3,000 ft (900 m) of slope and basin facies (Victorio Peak Formation and Bone Spring Formation, respectively, of King, 1942, 1965). At least 1,200 ft (360 m) of the Wolfcampian Hueco Group underlies the Leonardian deposits (Figure 3). These well-exposed Permian rocks are unconformably underlain by much less well exposed folded Carboniferous to Precambrian strata.

PREVIOUS WORK

Basic Permian stratigraphy of the Sierra Diablo was worked out by P. B. King in a classic study undertaken in the 1930's and published in 1942 and 1965 (King, 1942, 1965). This work stands today as a fundamental resource of geologic information on the

area. More recent work by Fitchen and others (1995) establishes the basic sequence stratigraphic framework architecture of the Wolfcampian Hueco Group and Leonardian Victorio Peak and Bone Spring Formations in the Apache Canyon area and provides an initial basis for relating outcrop studies to coeval subsurface producing Leonardian reservoirs of the Clear Fork and Wichita Groups. The work by Fitchen and others (1995; see also Fitchen, 1997) also establishes the Sierra Diablo as a fundamental research venue for characterization of Leonardian sequence stratigraphy and architecture. Preliminary reports on more detailed aspects of the geology of the Leonardian in the Sierra Diablo were published by Ariza (1998), Ruppel and others (2000), and Kerans and others (2000) and on petrophysics by Jennings and others (2000).

Other key insights into sedimentology and stratigraphy of the Leonardian in the Permian Basin region have come from subsurface investigations of shallow-water carbonate-platform reservoir successions in Texas. These studies, which have been based primarily on core and wireline-log data, include Mazzullo (1982), Ruppel, (1992), Atchley and others (1999), Ruppel (20002), and Ruppel and Jones (2007). A considerable amount of detailed biostratigraphic and more preliminary sedimentologic work has been also published on the coeval succession in the Glass Mountains of West Texas. Ross and Ross (2003) recently summarized this work from a sequence stratigraphic perspective. Unfortunately, detailed facies data are lacking for much of this succession, and access is now unavailable, making comparison with the Permian Basin succession problematic at best.

METHODS

Leonardian strata were studied along an approximately 2-mi (3-km) continuous outcrop on the south wall of Apache Canyon near the east margin of the Sierra Diablo (Figures 4, 5). Sixteen primary sections were measured and described foot by foot. Sections were tied into photomosaic panels that were prepared by merging outcrop photos obtained by ground and airborne photography. Correlations were established by walking out cycle contacts between sections wherever possible and tracing them onto photomosaics. Twelve supplementary sections located between primary sections were also described to constrain lateral facies and cycle relationships. Thin sections were collected in three of the primary sections to check facies identification. Additional stratigraphic sections were measured farther downdip in Marble Canyon (Figures 5, 6) to document the character and composition of equivalent platform-margin facies. Additional thin sections were prepared from 1,004 core plugs taken along vertical and horizontal traverses to measure petrophysical properties and to support facies definitions (using thin-section petrography). Porosity and permeability analyses are presented in Jennings and others (2000) and will not be considered further in this paper.

LEONARDIAN PLATFORM FACIES IN APACHE CANYON

Most of the Leonardian carbonate-platform rocks described in this work were assigned originally to the Victorio Peak Formation by King (1942, 1965). We have abandoned this usage for two reasons. First, recent studies in the nearby Guadalupe Mountains have shown that King's Victorio Peak includes part of the overlying San Andres Formation (Kerans and Fitchen, 1995; Kerans and Kempter, 2002). Second, our detailed studies in the Sierra Diablo demonstrate that the Victorio Peak can be subdivided into facies successions that are consistent with already-defined

lithostratigraphic units in the subsurface of the Permian Basin. Hence, in this paper we utilize these better-defined and

-understood subsurface names for the sections in Apache Canyon (Figure 7).

The Leonardian succession along the south wall of Apache Canyon, which includes all of the lower Clear Fork, the Tubb, and part of the lower upper Clear Fork of subsurface usage, measures as much as 400 ft (130 m) in thickness. This section includes about 160 ft (50 m) of lower Clear Fork, 40 ft (13 m) of Tubb, and 200 ft (65 m) of upper Clear Fork. Upper Clear Fork rocks are extremely well exposed along more than 2 mi (3 km) of outcrop, thus affording an opportunity for examining both large- and small-scale changes in facies, cyclicity, and petrophysics that cannot be observed in conventional outcrop or subsurface successions.

Ten major depositional facies have been defined in the Leonardian of the Sierra Diablos Canyon (Table 1). Each facies is interpreted to represent distinctive depositional conditions of wave energy, accommodation, and platform setting. Note that the entire Leonardian succession in the Sierra Diablos, like its counterpart in the subsurface of the Permian Basin, has been completely dolomitized. This dolomitization has obscured some of the fine textural details in these rocks, especially in fine-grained, mud-rich facies, but sufficient resolution of textures and fabrics remains to define major facies.

Table 1. Types and characteristics of major facies in Leonardian platform carbonates.

FACIES	Texture, fabric, & structure	Facies & systems tract	Cycle positior	Accommodati	Continuity
Tidal flat	Coated grains, intraclasts, cyano-bacterial lamination, fenestrae, isopachous cement; mudcracks, tepees, burrows,	Tidal flat; HST & TST,	Top	Very low	Very low
Silty mudstone-wackestone	Laminated to massive, burrowed	Basal **TST**	Base	Low	High
Ooid-peloid grain- dominated packstone & grainstone	Cross-laminated, to laminated, well sort	Ramp crest; **HST**, TST	Top	High	Locally high
Peloid grain- dominated packstone	Laminated, well sorted,	Ramp-crest, adjacent inner and ou platform; **HST**, TST	Top	High	Locally high
Peloid wackestone-packstone	Poorly sorted, burrowed	Inner platform; HST, TST		Low	High in the TST
Skeletal-peloid wackestone-packstone	Poorly sorted, burrowed, mollusks	Inner platform; HST, TST	Base	Low to high	Moderate
Fusulinid wackestone-packstone	Burrowed, nodular (dissolved sulfate nodules), open skeletal molds	Outer platform; HST, TST; middle platform; TST	Base	Low to high	High
Organic buildup	Irregular bedding and geometry	Outer platform; TST	NA	High	Very low
Crinoid/ brachiopod/ fusulinid wackestone-packstone	Poorly sorted	Distal, outer platform to slope's	NA	High	Moderate
Cherty mudstone	Fine-grained skeletal debris, chert masses; thin bedded	Distal, outer platform slope; TST	NA	High	High

Tidal-Flat Facies

These rocks contain a complex assemblage of textures, fabrics, and structures (Table 1). Most common are coated-grain/pisolite packstone, stromatolitic mudstone, and fenestral mudstone (Figure 8a, b). These grade laterally and vertically into an array of intermediate intermixtures of these sediments and other lithologies, including featureless mudstone, lithoclast breccia, and peloidal wackestone. Common to all of

these deposits is direct evidence of or association with indications of subaerial exposure. Although modern tidal flats contain subtidal, intertidal, and supratidal sediments (Shinn, 1983; Hardie and Shinn, 1986), only intertidal and supratidal sediments contain features that permit them to be identified reliably as belonging to the tidal flat. Accordingly, Clear Fork tidal-flat rocks exclude most subtidal rocks, although it is possible that such rocks may actually have been part of the tidal-flat complex. Because these rocks document exposure of the carbonate platform, this facies is a key indicator of platform accommodation and water depth and sea-level rise-and-fall history.

Silty Mudstone/Wackestone

Silty mudstone/wackestone rocks are characterized in outcrop by yellowish to pinkish color and presence of common small burrows (average 2–3 mm in diameter). Silt content is highly variable, commonly accounting for only 10 to 20 percent of the rock. Allochems are generally rare, although skeletal debris (chiefly mollusks) and peloids are locally present. These deposits are restricted essentially to the interval designated as the equivalent of the subsurface Tubb. Because of their silt content and muddy nature, these rocks typically weather recessively. Their generally covered outcrop expression, as well as their lithologic character, forms a readily definable break between platform-carbonate successions of the lower and upper Clear Fork.

Ooid, Grain-Dominated Packstone/Grainstone

As used herein, the term *grainstone* encompasses those rocks that are grain supported, contain little or no mud, exhibit interparticle pore space (either unfilled or filled), and display visible crossbedding. Rocks that possess all properties except

crossbedding are termed *grain-dominated packstones*. Because dolomitization commonly obscures bedding, as well as subtle textural details, these two rock types are not rigorously distinguishable.

The ooid, grain-dominated packstone/grainstone facies is composed of abundant well-sorted peloids, many of which are definable as ooids (Figure 8e, f). Grain size ranges from 150 to 350 microns. Where dolomitization obscures texture, ooids are distinguished by their larger grain size (fecal pellets are generally <150 microns). Most of these rocks in Apache Canyon display horizontal or low-angle cross-stratification. Skeletal grains are locally common; crinoids and fusulinids are common in basinward deposits, whereas bivalves and gastropods are found in more platformward settings. Modern ooids are formed in platform-margin settings, where relatively high wave energies are common (Ball, 1967; Harris, 1979). Presence of ooids, good sorting, and crossbedding and the near absence of mud indicate that deposition of the ooid, grain-dominated packstone/grainstone facies took place in well-agitated conditions.

Peloid, Grain-Dominated Packstone

These deposits are well-sorted, grain-supported rocks that contain visible carbonate mud and, like grainstones, exhibit interparticle pore space (either unfilled or filled). They grade into wackestone/packstone as mud content increases. Peloids comprise subspherical pellets that exhibit no discernable internal structure and most commonly range in size from 80 to 120 microns (Figure 8d). Ooids and skeletal debris are minor accessory grains in this facies. Most peloids are probably fecal pellets produced by infaunal, sediment-feeding organisms. However, some grains may be small ooids, eroded clasts of mudstone, or rounded skeletal fragments. Peloid, grain-

dominated packstone grades into skeletal, grain-dominated packstone with increasing skeletal content.

The fecal pellets that dominate this facies are produced by burrowing organisms in shallow-marine, mud-rich, generally low energy, inner-platform settings. In the modern Bahamas, for example, pelleted muds occupy broad expanses of the interior, wave-restricted platform of Andros Island (Purdy, 1963; Multer, 1977). Most of the pellets in these sediments, however, are poorly indurated and have little preservation potential during burial, their ancient rock equivalents being mudstones and pelleted mudstones (Milliman, 1974)—not the packstones of this facies. Some pelleted muds in these low-energy settings, however, undergo early lithification and can be preserved (Shinn and Robbin, 1983). It is these deposits that are the precursors of the pellet, grain-dominated packstone facies. These rocks thus owe their origins more to early diagenesis than to deposition in wave-agitated environments, as is the case with conventional packstones (Dunham, 1961). The excellent sorting observed in these rocks, which is a key to their good permeability in reservoir settings, is a function of the sizes of the organisms that produced them, rather than hydraulic processes. Causes of the early lithification of these pellets that is key to their preservation as “packstones” are not well understood. However, Beales (1965) suggested that cementation of such sediments is favored during sea-level-fall events.

Peloid Wackestone/Packstone

Peloid wackestone/packstone rocks are more mud-rich equivalents of peloid, grain-dominated packstones. Discernable peloids (which comprise both pellets and unidentifiable grains) are less abundant and commonly smaller, ranging from 120

microns to as small as 60 microns. Skeletal debris is locally present, most commonly consisting of mollusks. Pellets are generally well sorted. However, the abundance of mud indicates that sorting is not the result of wave action but rather a function of burrowing infauna. These rocks are found throughout lower and upper Clear Fork successions in Apache Canyon but are most common in more landward (west end of the south wall) settings. They probably were formed in low-energy, burrowed mud flats, much like those developed in the interior of Andros Island mud flats (Purdy, 1963; Multer, 1977).

Skeletal/Peloid Wackestone/Packstone

These rocks are similar and intergradational to peloid wackestone/packstones but contain substantially higher volumes of skeletal debris. Allochems commonly comprise restricted faunas (mollusks and rare calcareous algae), although small numbers of fusulinids and even rarer crinoids are locally present. Like the more-skeletal-poor, peloid wackestone/packstone facies, these rocks represent low-energy deposition across the platform.

Fusulinid Wackestone/Packstone

The fusulinid wackestone/packstone facies typically comprises abundant fusulinids and peloids (Figure 8c). Fusulinids generally average 2 to 3 mm in diameter and range in length from 5 to 20 mm. Their abundance ranges from about 10 percent to as much as 40 percent. Peloids are primarily fecal pellets produced by burrowing, as attested by their size and sorting. Fusulinid-bearing rocks are most abundant in the east

(depositionally downdip) parts of Apache Canyon and are dominant farther downdip in Marble and Mine Canyons. Studies of other Permian successions in the Permian Basin demonstrate that fusulinids are most common in relatively open marine waters on the outer part of the carbonate platform in water depths of approximately 30 m (Sonnenfeld, 1991). As such, fusulinid wackestone/packstone deposits represent the deepest water facies in most middle Permian successions. Accordingly, like the tidal-flat facies, which records the shallowest water setting, this facies is a key indicator facies of sea-level rise/fall history.

Organic-Rich Buildups

The deposits are restricted largely to the outer platform margin. Fitchen and others (1995) documented a succession of *Tubiphytes*-bryozoan-algal framestone in patch reefs along the platform margin (Figure 10). Such deposits are, however, rare in the middle and inner platform. Where present, they typically comprise thin, poorly bedded, organic-rich wackestones containing a diverse fauna of foraminifera, crinoids, fusulinids, and rare *Tubiphytes*.

Crinoid-Brachiopod-Fusulinid Wackestone-Packstone

Like the organic-rich buildups facies, crinoid-brachiopod-fusulinid wackestone-packstone rocks are restricted largely to the platform margin to slope. Fusulinids are most common in more proximal settings; crinoids and bryozoans are increasingly abundant downdip (Fitchen and others, 1995; Kerans and others, 2002; Ruppel and Jones, 2007).

Chert-Rich Mudstone

Chert-rich mudstones, which typify the Bone Spring Formation, are absent from all but the outermost reaches of the platform but are abundant in slope and basin settings. They typically crop out as poorly exposed, thin-bedded mudstones containing patches of silica, some of which can be identified as spiculitic, fine-grained, locally graded, skeletal debris and carbonate mud. Their lack of shallow-water fauna and parallel and graded bedding suggests that they were formed below storm wave base by mass gravity transport of fine-grained sediment fractions from the platform. In the study areas, they are restricted essentially to outer-platform to slope deposits at Marble Canyon (Figure 6), where they document backstepping during sea-level-rise-driven flooding events.

DEPOSITIONAL SETTING AND ACCOMMODATION

Leonardian platform facies in Apache Canyon are much like those documented for younger (Guadalupian-age) Permian successions (e.g., San Andres and Grayburg Formations) in the subsurface and in outcrops of the Permian Basin (Bebout, and others, 1987; Ruppel and Cander, 1988a, 1988b; Sonnenfeld, 1991; Kerans and others, 1994; Kerans and Fitchen, 1995). Kerans and Ruppel (1994) used interrelationships among these facies to construct a depositional model that relates facies to platform geography and accommodation (Figure 9). This model provides a basis for understanding spatial distribution of facies and facies tracts on the platform.

Four major platform facies tracts are represented in the model (Figure 9). The innermost platform is dominated by tidal-flat facies (fenestral mudstones, stromatolitic mudstones, and pisolite wackestone/packstones) that show evidence of frequent exposure and, thus, minimal platform accommodation. The middle platform is

characterized by mud-dominated facies (skeletal and peloidal wackestones) because of low accommodation (water depth) and low wave energy. Wave restriction in this setting is a function of distance from the open platform or position shoreward of the ramp crest. The ramp crest forms at the impingement point of open marine wave trains and thus occupies a relatively high energy setting. Ramp-crest facies are dominated by ooid grainstones and grain-dominated packstones. Parts of the ramp crest commonly aggrade to sea level, and capping tidal-flat deposits are locally common. In many cases, evidence of exposure and tidal-flat deposition is apparent at the top of ramp-crest successions. The outer platform marks the transition from shallow to deeper water conditions. This setting is dominated by fusulinid wackestone/packstones and locally by small buildups with associated crinoid wackestone/packstones.

Note that this model (Figure 9) is a composite of Permian platform facies tracts, not all of which are developed on the platform at all times. Ramp crests, for example, are best developed in high-accommodation, early highstand settings (Kerans and Fitchen, 1995); they are generally greatly reduced or absent in transgressive settings. Thus, this model is not designed to portray the detailed paleogeography at any discrete point in time. Instead, the model displays accommodation-based distribution of major facies types. As such, it provides a basis for understanding and interpreting accommodation-driven facies stacking patterns and cyclicity. For example, because most platform cycles are asymmetrical, upward-shallowing cycles (parasequences of some authors), cycle boundaries are defined by superposition of deeper water (higher accommodation) facies over shallower water (lower accommodation) facies. Inner-platform cycles can be defined by this kind of facies offset by superposition of subtidal facies over tidal-flat facies (minimum accommodation). Fusulinid-bearing rocks define

deepening and cycle bases in any succession of platform rocks (because they represent minimum platform accommodation) whenever they overlie other platform facies.

DIAGENESIS

All rocks in lower and upper Clear Fork successions in the study area have been dolomitized. As such, they are analogous to Leonardian carbonate-platform rocks that compose subsurface reservoirs in the Permian Basin. Although definitive studies of the diagenesis of Leonardian carbonates have not been completed, work to date suggests that most dolomites formed relatively early (Ye and Mazzullo, 1993; Saller and Henderson, 1998; Ruppel, 2002). Ruppel and Jones (2007) recently concluded that Clear Fork Group dolomites reflect both early cycle-top diagenesis and later Leonardian, sequence-punctuated, reflux dolomitization.

Although most dolomite is dominantly fine to medium grained (10–50 microns) and fabric retentive, textural characterization can be challenging. Facies definition requires careful examination of both outcrop features (grain size, bedding features, etc.) and thin-section petrography (grain size and pore variations).

Calcite is locally present in small amounts in dolomites from the south wall of Apache Canyon, but both distribution and character of these calcites suggest that their presence is due to later diagenesis. Some calcite is in the form of partial rims around open vugs. The optical character of these calcites and their occurrence suggest that many are due to partial replacement of anhydrite nodules. Other minor volumes of calcite cement encountered in these rocks may be the result of precipitation of meteoric calcite during Tertiary uplift of the Leonardian section. Studies of calcites in subsurface

cores have shown similar small volumes of calcite. The depleted-oxygen isotope signatures from these calcites tend to support a later meteoric origin (Kaufman, 1991; Ye and Mazzullo, 1993; Saller and Henderson, 1998; Ruppel and Jones, 2007).

The Leonardian platform succession in Apache Canyon differs principally from its subsurface counterpart in the absence of anhydrite. Calcium sulfate, mostly in the form of anhydrite, is abundant in most occurrences of Clear Fork rocks in the subsurface (Ye and Mazzullo, 1993; Saller and Henderson, 1998; Atchley and others, 1999; Ruppel, 2002; Ruppel and Jones, 2007). Absence of sulfate in outcrop probably attests to late dissolution and removal of anhydrite by meteoric waters. Presence of vugs in Apache Canyon outcrops, commonly the size of sulfate nodules observed in subsurface Clear Fork reservoirs, further supports this theory. The process of sulfate removal has no doubt been accentuated by uplift and exposure at the surface, but extensive sulfate dissolution has been reported by many workers in the subsurface of the Permian Basin (Lucia and Ruppel, 1996; Ruppel and Bebout, 2001).

SEQUENCE STRATIGRAPHIC SETTING

Work by Fitchen and others (1995; Fitchen, 1997) in Apache Canyon and subsequent work by Kerans and others (2002) in downdip areas of the canyon and by Ruppel (2002; Ruppel and Jones, 2007) in the subsurface of the Permian Basin indicate that the Leonardian comprises eight depositional sequences (Figure 7); four of these sequences are exposed in Apache Canyon (Figure 10). The extensive platform-to-basin exposures of Leonardian rocks in Apache Canyon allow a rare perspective of depositional architecture within two of these sequences that is usually available only with subsurface seismic data.

It is important to understand that in most cases, recognition of sequence boundaries is based on features of bedding geometry and erosion that are most readily defined at platform margins but not commonly apparent farther updip on the platform. Good examples are apparent in Apache Canyon. Stratal truncation and angular unconformities are apparent at the base of Leonardian sequences L1 (Wolfcamp/Leonard boundary) and L2 in Apache Canyon (Figure 10; Fitchen and others, 1995; Fitchen, 1997; Kerans and others, 2002). Toplap, indicative of forced regression, is similarly well expressed on the outer platform at the top of sequence L1 (Figure 10), but not readily apparent in middle and inner platform areas. Karst features (sinkholes, collapsed caves) are also most abundant on the outer platform (at the top of Sequence L1) and rare farther landward (Kerans and others, 2000). The top of Sequence L4, also a well-established regional sea-level-fall event, is expressed in Apache Canyon by a series of basinward-stepping wedges (Figure 10, Figure 6). This characteristic succession of stacked, basinward-stepping wedges can be identified readily on subsurface 2-D and 3-D data sets across much of the Permian Basin, providing a ready basis for correlations between outcrops and the subsurface and documenting the widespread nature of this sea-level-fall event. (Figure 11). Despite the marked evidence of sea-level fall and rise apparent at each of these sequence boundaries in outer-platform to slope areas, recognition of equivalent surfaces is commonly problematic in more landward areas of the carbonate platform. This study documents the effects of sea-level changes in inner- to middle-platform areas, where sequence boundaries are not generally definable from changes in stratal architecture.

Two things are apparent from the excellent outcrops of Leonardian platform-margin and slope outcrops in Apache Canyon. First, the character of Leonardian

sequence boundaries varies substantially both in terms of geometric relationships and facies. Second, the large-scale relationships necessary to define these boundary geometries, although commonly well expressed at the platform margin and slope, are commonly not apparent in more proximal settings of the platform. The remainder of this paper focuses on two fundamental questions that have implications for characterization and interpretation of all Leonardian carbonate platforms: (1) Can classically defined Leonardian sequence boundaries be identified in carbonate-platform areas? And (2) if not, what record of eustatic control of sediment accumulation can be defined in these areas, if any?

CYCLE AND SEQUENCE STRATIGRAPHY OF LEONARDIAN PLATFORM DEPOSITS AT APACHE CANYON

All of Leonardian sequence L2 and most of Leonardian sequence L3 are prominently and extensively exposed in the interior reaches of Apache Canyon (Figures 10, 12). The continuity of these world-class outcrops makes it possible to examine lateral and vertical patterns of facies stacking and to characterize styles of higher frequency cyclicity and facies-tract development. Two such higher frequency scales of cyclicity are apparent: depositional cycles and high-frequency sequences. As used herein, the term *cycle* refers to repetitive stacks of predominantly upward shallowing facies successions. Most such cycles in Apache Canyon are 1 to 2 m in thickness and traceable over several kilometers. As such, they are considered to be equivalent to parasequences or high-frequency cycles of some authors.

High-frequency sequences (sensu Kerans and Fitchen, 1995; Kerans and Kempter, 2002) are essentially transgressive-regressive successions that record intermediate-scale (between cycle and sequence scale) sea-level rise, aggradation, and

relative sea-level fall on the platform. As we will demonstrate, high-frequency sequences (HFS's) constitute a critical level of stratigraphic hierarchy in Leonardian carbonate platforms that is not readily predictable from sequence boundaries defined in outcrops or in the subsurface. This fact is well illustrated in the seismic-scale outcrops in Apache Canyon.

Leonardian 2: Lower Clear Fork Sequence Architecture

The base of Leonardian sequence L2 is well defined at the platform margin and slope by basal onlapping beds overlying the prominent toplap bed geometries and erosion at top of sequence L1 (Figure 10). This sequence boundary, however, is much more cryptic on the platform. The top of L1 is also marked on outer reaches of the platform by local karsting (Kerans and others, 2000). In these areas of cave and sinkhole collapse, the sequence boundary is well defined by its relatively sharp and undulating, unconformable surface topography and by local infilling of karst depressions by basal L2 facies (Figure 13). Across most of the more proximal parts of the platform, however, karsting is rare, and the sequence boundary is less easily defined. In these areas, the base of L2 is defined primarily by facies-tract offset; transgressive inner-ramp, tidal-flat facies of the basal L2 sequence overlie outer-ramp facies of the topmost L1 sequence. Such facies-tract offsets (formed either by superposition of markedly shallower facies overlying deeper water facies, as seen here, or by the more common superposition of deeper water facies over shallower facies) are typically the primary basis for sequence-boundary definition in platform interior areas.

The remainder of L2 is characterized on the outer platform by dominantly aggradational facies stacking (Figure 10; Fitchen and others, 1995). Farther landward,

however, L2 facies stacking patterns document several higher frequency, transgressive-regressive successions (Ariza, 1998). These successions define three high-frequency sequences (Figure 12). Two of these HFS's (basal, HFS 2.1, and middle, HFS 2.2) consist of typical symmetrical facies-tract successions, including a basal, transgressive leg of tidal-flat facies, a middle leg of subtidal facies representing maximum flooding during early highstand, and an upper leg of tidal-flat facies representing late highstand filling of accommodation. HFS 2.3 differs from HFS 2.1 and 2.2 by being asymmetric (upward deepening) in its internal architecture. Although basal transgressive and maximum flooding legs are well represented in this HFS, there is no evidence of late highstand aggradation or shallowing. Instead, the top of HFS 2.3 comprises outer-platform fusulinid wackestones and peloid-ooid packstones. Absence of late highstand deposits at the top of HFS 2.3 here, combined with the presence of toplapping bed geometries at the top of sequence L.2 farther downdip (Figure 10; Fitchen and others, 1995; Kerans and others, 2000), suggests that the absence of fully aggraded highstand deposits may be due to forced local regression. In a recent study of sequence L2 in the subsurface of the Permian Basin, for example, Ruppel and Jones (2007) documented four HFS's, each bearing fully aggraded, late highstand deposits at their tops with no indication of forced regression. This suggests that the upper L2 architecture in Apache Canyon (i.e., within HFS 2.3) may be a function of local tectonic movement in the Sierra Diablo area rather than a product of regional eustatic causes alone.

It is important to note that facies-based definition of HFS is best performed in mid- to outer-platform settings, where a complete accommodation history is recorded (middle and east parts of section; Figure 12). In platform interiors, accommodation is commonly low, even during maximum platform flooding. Note also that more updip

areas of Apache Canyon (west part of section; Figure 12) contain dominantly tidal flat facies. In such areas, interpretation of facies-tract offsets can be misleading as to true accommodation history. For example, a measured section at the west end of the Apache Canyon field area would lead to an interpretation of sequence boundaries different from that of a section at the east end.

The quality of lower Clear Fork (L2) equivalent outcrops in Apache Canyon is generally poorer than that of underlying Abo (L1) or overlying upper Clear Fork (L3) deposits. This is largely a result of the dominance of less-well-exposed tidal-flat and other mud-rich inner-ramp facies in the lower Clear Fork. These incomplete exposures limit the resolution of cycle-scale facies stacking patterns. Nevertheless, critical sequence stratigraphic relationships are clearly definable. Most significant of these are accommodation-driven facies stacking patterns in L2 HFS (L2.1 and L2.2). These relationships (a symmetrical, shallow-water to maximum-flooding to shallow-water accommodation trend for L2.1 and an asymmetrical shallow-water to deepening facies succession for L2.2) provide a basic model for interpreting and modeling subsurface reservoirs in the Permian Basin.

Leonardian 3: Upper Clear Fork Sequence Architecture

Although the L3 sequence is stratigraphically incomplete owing to erosion, it is much better exposed along the length of Apache Canyon than is the underlying L2 sequence. As a result, outcrops give a detailed picture of high-frequency sequence architecture that is not apparent in more basinward successions.

Outcrop studies in Apache Canyon support interpretations made using subsurface data sets (e.g., Ruppel and Jones, 2007) that the boundary between

Leonardian sequences L2 and L3 is at the base of a silt-rich, dominantly covered interval (Figures 3, 10, 12). In the subsurface, these silt-rich rocks are assigned to the Tubb Formation (Figure 7). Although the base of the Tubb interval is poorly exposed in most outcrop sections, locally there is evidence of truncation and possible karsting below this surface (Fitchen and others, 1995; C. Kerans, personal communication, 2006). In addition, a sharp contrast in facies (i.e., facies offset) exists between the open-marine, outer-platform fusulinid wackestones and peloid-ooid packstones at the top of sequence L2 (HFS 2.3) and the silt-rich, shallow-water mudstones, wackestones, and tidal-flat capped cycles of the Tubb succession at the base of sequence L3 (Figure 12). Placement of the Tubb at the base of a major sequence is also consistent with clastic sediment distribution patterns observed throughout the Permian in the Permian Basin. Many authors have recognized that Tubb siliciclastics correlate to basinal siltstone successions and together define a period of shelf transport of aeolian clastics across the exposed L2 platform during sea-level lowstand (Mazzullo and Reid, 1989; Ruppel and Bebout, 2001; Kerans and Kempter, 2002; Barnaby and Ward, 2007).

In spite of partial erosional truncation, three high-frequency sequences (HFS's) and part of a fourth are definable within L3 along the south wall of Apache Canyon, based on facies tract offsets (Figure 12). The basal, high-frequency sequence, HFS 3.1, comprises the recessively weathering, siliciclastic-rich Tubb succession. HFS 3.2, 3.3, and 3.4 are composed entirely of carbonate-platform sediments (Figure 12). The lower two HFS's (3.1 and 3.2) have well-defined transgressive bases and highstand tops; the third (3.3) contains only a transgressive base, the top having been removed by modern erosion. Patterns of facies and sequence offsets in the exposed L3 section on the south

wall of Apache Canyon indicate that all three HFS's are part of the transgressive, or backstepping, leg of L3.

HFS 3.1

The basal HFS of L3, which reaches a maximum thickness of approximately 35 to 40 ft (8 to 13 m), documents renewed transgression of the Clear Fork platform following sea-level fall at the end of L2. By analogy with subsurface successions, this siliciclastic-rich HFS is assigned to the Tubb Formation. The Tubb is readily correlatable throughout the platform-top areas of Apache Canyon by its recessive weathering profile that separates the more resistant, cliff-forming carbonate successions of both the underlying L2 lower Clear Fork and overlying L3 upper Clear Fork (Figure 3).

Although largely covered, scattered exposures of the Tubb indicate that it consists dominantly of siltstone-based cycles, the lowermost of which possess peritidal caps. These high-frequency, exposure-capped cycles document gradual low-accommodation transgression associated with initial L3 sea-level rise. Cycles in the upper Tubb contain more normal marine peloidal and skeletal packstone, reflecting a gradual increase in accommodation. Fitchen and others (1995) showed that Tubb siliciclastic-rich peritidal facies pass downdip into dominantly subtidal deposits of siltstone and sandstone.

HFS 3.2

HFS 3.2 comprises five distinct facies tracts, all dominated by carbonate sediments, including (1) a basal transgressive, low-accommodation TST succession; (2) a maximum flooding to early HST outer-platform succession; (4) a middle-platform,

maximum flooding to early HST ramp crest; (5) a maximum flooding to early HST inner platform; and (6) a sequence-capping, low-accommodation, late HST exposed-platform-top succession.

The TST succession consists of cycles composed of basal fusulinid wackestone and capping grain-dominated peloid packstone (Figure 12). These rocks, which represent the basal upper Clear Fork Formation, are low-accommodation sediments that accumulated during slow transgression in a relatively low energy setting. Reflecting their stable interior platform setting, these deposits are isopachous and continuous over broad expanses of the platform.

HFS 3.2 transgressive systems tract deposits are overlain by progressively higher energy, coarser grained, ooid-peloid, grain-dominated packstones and grainstones of the HFS 3.2 highstand systems tract. To the east, and possibly at least obliquely down depositional dip, these deposits pass into a thick amalgamated succession of ooid grainstones of the ramp crest (Figure 12). Farther northeast and more clearly downdip, high-energy ramp-crest deposits are replaced by fusulinid-based cycles typical of the outer ramp (Figure 12).

In contrast to the continuity of low-accommodation TST deposits of the basal HFS 3.2, there is considerable lateral facies variability in the overlying maximum flooding and highstand legs. Three distinct facies tracts are apparent: an updip or landward inner-ramp succession, a downdip or basinward outer-ramp succession, and an intervening ramp-crest succession (Figure 12). The inner ramp is characterized by weakly cyclic, mud-rich peloid packstones and wackestones; the ramp crest by amalgamated, peloid-ooid packstones and grain-dominated packstones; and the outer

ramp by fusulinid-based and peloid packstone-capped cycles. An extensive tidal-flat succession forms the top of the inner-ramp and ramp-crest successions.

The top of HFS 3.1 is best defined in the ramp-crest area. In this area, renewed sea-level rise is documented by the superposition of outer-ramp, fusulinid-bearing cycles over ramp-crest grainstone, with incipient fenestrae and a thin, peritidal cap. This facies-tract offset is much less apparent both downdip and updip, making the sequence boundary much more cryptic in these areas. Outcrop tracing of the HFS boundary shows that in the inner-ramp area, the top of HFS 3.1 lies within a thick section of tidal-flat deposits (Figure 12). It is apparent that tidal flats developed during both the late 3.2 highstand and during early transgression of the overlying 3.3. Without 2-D outcrop control and traceable outcrop sections, this sequence boundary would probably be mistakenly placed at the top of the tidal-flat succession (that is, in the base of HFS 3.3).

In outer-ramp areas, recognition of this HFS boundary is similarly difficult. There, peloid-ooid packstone-grainstone-capped cycles of the 3.2 highstand outer-ramp succession are overlain by somewhat muddier and finer grained but similar peloidal packstones of the basal HFS 3.3. But no marked surface or facies-tract offset is easily definable.

HFS 3.3

The internal sequence architecture of HFS 3.3 is similar to that of 3.2, comprising a basal transgressive ramp succession overlain by accommodation-controlled outer-ramp, ramp-crest, and inner-ramp facies tracts. The primary difference between the two is the absence of a well-developed tidal-flat succession at the top of 3.3. However, there are also differences in the transgressive legs of the two sequences that probably reflect

inherited accommodation patterns on the platform. Unlike HFS 3.2, HFS 3.3 transgressive deposits are clearly differentiated into inner- and outer-platform facies tracts: a high-accommodation, transgressive systems tract (TST), subtidal ramp downdip and a low-accommodation, tidal-flat succession updip (Figure 12). Facies-tract differentiation during 3.3 transgression probably reflects platform accommodation trends inherited from sedimentation patterns during HFS 3.2. The presence of thicker and more continuous fusulinid deposits in the transgressive leg of HFS 3.3 (compared with 3.2) indicates higher accommodation flooding and deposition, probably a result of continued, longer term (sequence-scale) sea-level rise.

The base of HFS 3.3 is defined by facies offset along the 2-D dip section. This offset is particularly easy to recognize above the 3.2 ramp crest, where high-energy ooid/peloid packstones and grainstones are overlain by lower energy skeletal (fusulinid/mollusks) wackestones representative of renewed flooding and sea-level rise. As described earlier, the basal HFS 3.3 contact is much more difficult to define in more landward tidal-flat areas, where tidal-flat facies of HFS 3.3 overlie HFS 3.2 tidal-flat deposits. For the most part, however, highstand-exposure facies at the top of HFS 3.2 comprise pisolitic, grain-dominated packstones and other diagenetically overprinted subtidal deposits. By contrast, basal transgressive HFS 3.3 deposits more commonly contain laminated, fenestral, mud-dominated, tidal-flat facies.

Although 2-D relationships indicate that the HFS 3.2–3.3 boundary lies well below the top of the tidal-flat complex (see Figure 12), the sharp erosional contact that exists at the top of these tidal-flat deposits would probably be selected by most workers to be the sequence boundary in 1-D or limited 2-D sections. This surface, which displays erosional truncation of underlying beds and development of small solution pits

is a marine flooding surface that separates underlying, exposed, tidal-flat rocks from overlying, subtidal, fusulinid-bearing wackestone-packstone. Presence of this sharp contact above the true sequence boundary demonstrates the care that must be taken to define the sequence stratigraphy of carbonate-platform successions accurately.

Inner- and outer-ramp facies tracts in HFS 3.3 are similar in facies composition and cyclicity to those of HFS 3.2. The 3.3 ramp-crest facies tract, however, differs from that of 3.2 in being more ooid rich. The greater abundance of ooids in 3.3 is consistent with an upward increase in accommodation and energy associated with continuing transgression through Leonardian sequence L3.

The upper boundary of HFS 3.3 is similar to the upper boundary of 3.2. The contact with HFS 3.4 is best defined in the ramp-crest area, where ramp-crest ooid-peloid grainstones and packstones are overlain by outer-ramp fusulinid wackestones. Like the marine flooding surface near the base of 3.3, this surface of facies offset displays erosional truncation and solution pitting of the underlying rocks. In inner- and outer-ramp areas, the contact is again more cryptic. There is no HFS-capping tidal flat at the top of HFS 3.3, nor is there a basal tidal-flat succession at the base of HFS 3.4. Absence of exposure-related facies development here probably reflects the progressive westward (landward) flooding of the platform and a continuing increase in long-term accommodation. HFS boundary, tidal-flat deposits would probably be encountered farther east, had these deposits not been removed by modern erosion.

HFS 3.4

HFS 3.4 is truncated partly by modern erosion along the south wall of Apache Canyon. The transgressive leg of HFS 3.4 is exposed, but only in the east, more

basinward, parts of the canyon (Figure 12). As discussed earlier, the base of the HFS is indicated by a sharp erosional contact and facies offset between ooid grainstone and grain-dominated packstone cycles of the upper HFS 3.3 and overlying basal fusulinid-dominated cycles of HFS 3.4. This surface, which resembles the marine flooding surface in the lower TST of HFS 3.3, displays development of karst pits and as much as 3 ft (1 m) of relief. Although the contact between HFS 3.3 and 3.4 is less dramatic basinward, an obvious increase in accommodation is definable by the presence of abundant fusulinids at the base of HFS 3.4. Eastward (down depositional dip), these outer-ramp cycles become dominated increasingly by crinoids and brachiopods. Although the upper part of HFS 3.4 is missing, thickness of outer-ramp, fusulinid-rich, TST deposits compared with that of underlying sequences suggests that 3.4 represents continued long-term sea-level rise and increasing accommodation. It is likely, but impossible to prove in these outcrops, that 3.4 represents maximum flooding of the platform during L3.

CYCLICITY AND CYCLE STACKING PATTERNS

Leonardian platform outcrops in Apache Canyon offer important insights into cycle composition and cycle stacking patterns that are useful in describing and interpreting outcrop and subsurface successions elsewhere in the region. Study of these outcrops reveals that cyclicity, facies stacking patterns, and cycle continuity vary among facies tracts. In tidal-flat-capped successions and less commonly in subtidal successions, 3- to 6-ft-thick (1- to 2-m-thick) cycles are definable in vertical sections but are generally not correlatable. However, subtidal cycle bundles, which average 15 to 30 ft (5 to 9 m) in thickness, can be correlated widely. These bundles typically consist of

upward-shallowing successions of basal skeletal wackestones and capping peloid-ooid packstones.

Transgressive Systems Tract Cyclicity

Facies stacking patterns in Clear Fork transgressive systems tracts vary according to accommodation. High-accommodation TST cycles (Figure 14) are typical of outer-platform settings. In Apache Canyon, these cycles are well developed in distal parts of HFS 3.2, 3.3, and 3.4 (in the east part of the canyon). These cycles have fusulinid wackestone-packstone bases and ooid-peloid, grain-dominated packstone tops (Figure 15C2). Commonly, cycle tops are strongly burrowed, making precise delineation of cycle boundaries difficult because of admixing of sediments from the overlying cycle into cycle-top deposits. In more proximal settings, especially in or near the ramp crest, cycle tops may comprise high-energy grainstones containing mixtures of ooids, peloids, and skeletal debris; cycle bases are typically finer grained peloid packstones, with scattered skeletal debris (Figure 15C3). In some instances, ramp-crest cycles are amalgamated, although this is most common in highstand successions.

Low-accommodation TST cycles differ from those just described principally in being more mud rich and finer grained. These deposits are developed characteristically in more proximal platform settings during early transgression. Low-accommodation subtidal cycles are lower energy, updip equivalents of the high-accommodation cycles of the outer ramp discussed earlier. These cycles, which are best developed in the transgressive leg of HFS 3.2 (basal upper Clear Fork), are characterized by skeletal-rich bases and peloidal tops (Figures 15C1 and 16). Cycle boundaries are gradational and symmetrical: typical of subtidal transgressive cycles. Continuity of these cycles is

among the highest in the Clear Fork. Individual cycles can be traced for more than 1.5 mi (2.5 km) along the outcrop. Textural contrast between cycle base and top is small, however. Accordingly, these cycles may not express systematic petrophysical differences in subsurface reservoirs.

More updip, low-accommodation TST cycles are dominated by tidal-flat successions. These cycles typically comprise peloidal mudstone-wackestone bases and exposure caps (Figure 15A1). Such cycles characterize basal deposits of HFS 2.1 and 2.2 (lower Clear Fork) in Apache Canyon. These cycles are commonly difficult to distinguish from exposure cycles found in highstand settings—for example, at the top of HFS 3.2 (Figures 15A2 and 12).

Highstand Systems Tract Cyclicity

Typical highstand systems tracts (HST) are poorly developed in low-accommodation HFS's at Apache Canyon (HFS 2.1 and 2.2 are low-accommodation HFS's in the study area). However, they are well represented in the upper legs of Leonardian HFS 3.2 and 3.3 (Figure 12). Two types of HST cycles are dominant (Figure 15B1 and 15B2). Cycles in distal or open-ramp settings contain peloidal-skeletal, packstone-grain-dominated packstone bases and ooid-peloid, grain-dominated packstone tops (Figure 15B1). Although similar to distal-ramp TST cycles (Figure 15C2), these cycles differ in containing only rare fusulinids. Instead, they contain a mixed skeletal complement of mollusks, brachiopods, and crinoids. Cycle-base facies are typically highly burrowed and weather to rough irregular surfaces.

Proximal HST cycles reflect higher energy conditions of the ramp crest. They typically comprise amalgamated grain-dominated packstone to grainstone successions

(Figure 15B2). Cycle boundaries are commonly difficult to define, although locally they are marked by vertical burrows that contain skeletal sediment fill (Figure 15B2). These cycles are common in the highstand ramp crests of HFS 3.2 and 3.3 (Figure 12).

Terminal HST cycles display the effects of overprinting early diagenesis related to exposure during late highstand and ensuing sea-level fall. These cycles, which are common in the top of HFS 3.2 in Apache Canyon overlying and landward of the ramp crest (Figure 12), are locally difficult to distinguish from tidal-flat deposits. Most, however, are composed of ooid-peloid, grain-dominated packstones to grainstones that display pisolite formation and development of keystone vugs in exposed, high-energy, ramp-crest deposits (Figure 15A2).

Cycle and Facies Continuity

Facies continuity is greatest in Leonardian TST successions. It is especially apparent in basal TST cycles of HFS 3.2 and HFS 3.3. In both, basal transgressive cycles and component facies can be traced for more than 1 mi (1.6 km) along the south wall of Apache Canyon. Although facies undergo minor changes in allochem content (principally a basinward increase in cycle-base fusulinid content), cycles are correlative throughout this distance (Figure 17). In the case of HFS 3.2, cycle continuity is consistent with flooding a relatively flat topped platform. This conclusion is supported by the character and continuity of the siliciclastic-rich cycles of the underlying Tubb succession. Character of these low-accommodation transgressive cycles is displayed in Figure 17. Weathering patterns (Figure 16) permit these cycles to be traced along the entire length of the outcrop.

Cycle continuity is also excellent in the transgressive leg of HFS 3.3, which is surprising considering the depositional relief developed during HFS 3.2 highstand indicated by the downdip change from exposure-overprinted ramp-crest to outer-ramp deposits (Figure 12). Good continuity in TST deposits suggests that this relief was filled by early TST deposition along the outer ramp before highly continuous TST cycles were deposited. Figure 18 depicts cycle development and continuity in HFS 3.3 transgressive deposits and in the overlying ramp crest at the turnaround from TST to highstand. The basal cycle of this set of cycles (part of the TST) displays nearly constant facies stacking relationships along more than 1 mi (1.6 km) of outcrop exposure. The overlying early highstand cycles, however, display less lateral continuity because of amalgamation of cycles and facies in ramp-crest areas.

Cycle Definition and Correlation

Facies relationships expressed in the Leonardian in Apache Canyon offer important insights and caveats to recognizing and defining cycles in subsurface Clear Fork Group successions. It is significant that the styles of cyclicity and internal facies stacking patterns exhibited here are consistent with and similar to styles documented from outcrop studies of younger Permian (Guadalupian) reservoir successions (Sonnenfeld, 1991; Kerans and others, 1994; Kerans and Fitchen, 1995; Barnaby and Ward, 2007). This fact is perhaps somewhat surprising, considering how difficult cycle recognition and correlation have proven to be in many Clear Fork subsurface reservoir successions. Nevertheless, basic facies stacking patterns are consistent with models of Permian depositional environments and paleogeography developed from studies of Guadalupian outcrops and reservoirs (Figure 9). Some deviations to standard Permian

cycle styles are apparent in the Leonardian of Apache Canyon, however, that make cycle definition and recognition difficult.

In contrast to Guadalupian cycles, Leonardian cycles appear to be dominated by lower energy deposition. This is supported by the rarity of ooid-rich grainstones and the dominance of peloidal wackestones and packstones. Because of the prevalence of lower energy conditions, cycle boundaries are commonly gradational and more difficult to define. Throughout most of the Leonardian Clear Fork succession in Apache Canyon, cycles are best defined by contrasts in skeletal and nonskeletal allochems. In general, subtidal cycles are composed of poorly sorted, skeletal-rich, burrowed, muddier bases and well-sorted, skeletal-poor, peloid- to ooid-rich tops. Key indicators of cycle definition in these rocks are thus sorting, skeletal distribution, burrowing, and grain size.

Infaunal burrowers have contributed significantly to Leonardian depositional processes, as is evident from the abundant pellets in these shallow-water-platform sediments. Although much of the burrowing is associated with slower rates of sedimentation in cycle-base facies, burrows are also common at cycle and bed contacts. Presence of abundant burrows in cycle bases enhances their outcrop recognition by creating distinctive weathering styles (Figures 14, 15). Vertical burrowing at cycle and bed tops, however, produces intermixtures of textures and sediment types that make positioning of cycle boundaries difficult. For example, in many cases, fusulinids and other skeletal debris are admixed into cycle-top facies (Figure 15B). In other words, cycle tops may contain common to abundant skeletal material as a result of postcycle burrowing.

Cycle and Facies-Tract Dimensions

Styles of cycle development vary systematically among facies tracts. Aspects of these variations that have potential significance in defining reservoir flow properties include facies-tract width, cycle continuity, cycle thickness, and textural contrast. Each of these can be measured in the L3 (upper Clear Fork) succession of continuous outcrops along the south wall of Apache Canyon (Table 2).

Table 2. Properties of Leonardian Clear Fork platform cycles and facies tracts.

Facies tract	Tract width	Cycle continuity	Cycle thickness	Textural contrast
Low-accommodation TST platform	Thousands of feet (>5,000)	Width of facies tract	5–10 ft (2–3 m)	Subtle
High -accommodation TST platform	Thousands of feet (>5,000)	Width of facies tract	10 ft (3 m)	Marked
Outer-platform HST	Thousands of feet (>2,000)	Width of facies tract	5–10 ft (2–3 m)	Marked
Low-energy Inner-platform HST	Thousands of feet (>3,000)	Variable (<2,000 ft)	10–20 ft (3–6 m)	Variable
Ramp crest	Narrow (<2,000)	Variable	Variable 10–20 ft (3	Variable
Tidal-flat TST, HST	Thousands of feet (>5,000)	Very limited	2–6 ft (1–2 m)	Variable

Because facies tracts have relatively consistent styles of cycle development and continuity, knowledge of the extent of both cycles and facies tracts can be important in developing depositional models, as well as models for fluid flow. Outcrops along the south wall of Apache Canyon probably extend in a direction that is somewhat oblique to depositional dip; dip versus strike dimensions are therefore not certain. Measures of facies-tract width and cycle extent (continuity) from Apache Canyon outcrops are nevertheless valuable because, in most cases, depositional strike and dip are even less well known in more conventional (i.e., smaller) outcrops, as well as in the subsurface. Knowledge of cycle thicknesses and textural contrast is important for developing a basis for defining cycles and component facies and interpreting and modeling vertical

permeability. As used here, textural contrast refers to that found at cycle boundaries. If great, this contrast can be the basis of marked vertical changes in permeability.

Both low-accommodation and high-accommodation TST tracts have large lateral extents. This seems to be best explained by the relative flatness of the antecedent platform and resulting widespread similarity of accommodation conditions across the platform during transgression. In Apache Canyon, TST facies tracts can be traced for at least 5,000 ft (1500 m)—length of the studied outcrop. It is possible that their true extent is far greater. Individual cycles can be traced for the full extent of these TST facies tracts. It is, in fact, cycle continuity (demonstrated by actual tracing of cycles on photomosaics) that defines the extent of the facies tract. Cycle thicknesses are similar in both low- and high-accommodation TST tracts, although, not surprisingly, they appear to be slightly thicker in the latter. The textural contrast between component facies (at cycle boundaries and within cycles) is substantially greater in the high-accommodation TST—a result of higher energy conditions associated with higher accommodation settings, even in basal HFS TST tracts.

Highstand facies tracts are generally shorter, and they possess more variable properties of cycle continuity, thickness, and textural contrast (Figure 15B; Table 2). This reflects the partitioning of the platform during highstand by wave- and energy-related carbonate deposition. In terms of facies tract dimensions, the Clear Fork ramp crest is especially noteworthy in that it displays a dip dimension of as short as 2,000 ft (600 m) or less (Figure 12). This is particularly significant when it is considered that facies of the ramp crest (ooid/peloid, grain-dominated packstones and grainstones) are potentially the most porous and permeable in the succession. Outer- and inner-platform tracts have significantly greater dip extents, being limited by the platform margin and

updip strandline, respectively. Cycle continuity and textural contrast in the outer-platform HST are similar to that found in the high-accommodation TST; this is due to the similarity in cycle composition and facies stacking between the two tracts. By contrast, these properties vary substantially in ramp crest and inner platform. In the case of the former, this is a result of local, cycle amalgamation. On updip and downdip margins of the ramp crest, cycles display good continuity and strong textural contrast at cycle boundaries. In the high-energy center of the ramp crest, however, some muddier subtidal bases are absent, resulting in reduced textural contrast at cycle boundaries and an apparent thickening of cycles. In the inner-platform cycle, continuity is difficult to define because of the low contrast in dominantly muddy facies.

Late HST and early TST tidal-flat tracts also exhibit rather extensive facies-tract development (Table 2). In Apache Canyon, HST tidal-flat facies extend updip beyond the study area (at least 5,000 ft; 1500 m). Cycles in the tidal-flat tract are thinner than in other tracts (Figure 15A; Table 2), and continuity is the lowest in the Clear Fork outcrop succession. Accordingly, textural contrast across cycle boundaries is variable and unpredictable, reflecting widely varying conditions on the tidal flat and resulting heterogeneous array of sediment types.

DISCUSSION

Outcrops in the Sierra Diablo provide important insights into styles of cyclicity, sequence development, and stratigraphic architecture of Leonardian carbonate platforms. Not surprisingly, Leonardian platform rocks in the Sierra Diablo display accommodation features intermediate between those characteristic of underlying Upper Carboniferous – Lower Permian ice-house successions and overlying greenhouse

rocks. Unlike ice-house successions, Leonardian cycles and high-frequency sequences are typically fully aggraded, many being capped by exposure-related facies (Figure 15). Cycles rarely display evidence of karst-related diagenesis at their tops like their colder climate counterparts. Instead, karsting is restricted to longer duration sea level falls marked by composite sequence boundaries.

Perhaps most significant is the nature of high-frequency sequence (HFS) development within composite (3rd-order) sequences. Although composite sequences are best (and perhaps only) defined at the platform margin and slope, these high-frequency sequences can be defined only on platform tops. Patterns of TST and HST systems-tract development in these HFS's define the basic depositional architecture that most likely exists on many such platforms. These architectural elements are particularly well expressed in Leonardian sequence L3. HFS 3.2 and 3.3 display facies characteristics, styles of cyclicity, and facies stacking patterns in outer-platform, ramp-crest, and inner-platform facies tracts. Together with overlying HFS 3.4, these two HFS's also clearly demonstrate accommodation-driven changes in geometry, such as landward offset, facies-tract thickness changes, and facies composition changes that are associated with longer-term sea-level rise. Because most carbonate outcrops and subsurface reservoir successions record platform-top deposition, these relationships offer important lessons in interpreting 1-D and less-comprehensive 2-D data sets in such settings.

In parts of the platform top, HFS boundaries can commonly be defined by simple facies offset. This technique is most reliable in ramp-crest and proximal outer-platform areas along a dip transect (e.g., tops of HFS 3.2 and 3.3; Figure 12). By contrast, in proximal ramp-crest and inner-platform settings, facies offsets can be lacking or

misleading. For example, the top of HFS 3.2 would be erroneously defined too high (in the TST of HFS 3.3) if facies offset alone were used in the Apache Canyon dip section (Figure 12). The actual position of the sequence boundary is in the middle of the tidal-flat facies succession that straddles the boundary between 3.2 and 3.3 (Figure 12). Unfortunately, identifying sequence boundaries in such a "sequence boundary zone" (sensu Osleger and Read, 1991; Montanez and Osleger, 1993; Osleger and Montanez, 1996) is difficult in most outcrops and subsurface data sets, where lateral correlations can generally only be inferred not proven (by walking out bedding planes). In such situations, it is likely that the HFS boundary would be miscorrelated to extend from the top of the tidal-flat facies in the inner platform to the facies offset defined in the outer platform. Apache Canyon outcrops illustrate some caveats that should be noted when attempting sequence-boundary correlation from more limited data sets.

Contrasts in sequence facies architecture and thickness between L2 and L3 offer insights into longer-term accommodation controls on platform sedimentation. The less-thick, irregular distribution of grain-rich facies and generally less well differentiated facies tracts in L2 suggest that a true ramp crest may not have developed during L2. Subsurface Permian Basin data sets exhibit similarly thinned L2 thickness, limited development of L2 ramp crests relative to L3, supporting this interpretation (Ruppel and Jones, 2007). Presence of thicker successions and better developed ramp crests in L3 suggests increased, longer term (2^{nd}-order) accommodation from L2 to L3 (Figure 12).

Patterns of facies development and stacking in Apache Canyon outcrops offer valuable lessons in identifying cycle boundaries in 1-D data sets. Evidence of infaunal burrowing is abundant throughout the succession in the form of abundant fecal pellets, but identifiable burrow traces are especially apparent in high-accommodation and grain-

rich highstand facies successions (Figure 15B). Variations in burrow abundance probably reflect, to some degree, types of organisms active in each setting, but they also seem to be a function of preservation potential; burrow fillings are most readily identifiable where facies contrasts are greatest (i.e., in grain-rich facies stacks). Burrows are commonly developed at cycle tops and can serve as an important tool in identifying the cycle boundary (e.g., Figures 15C2, 3). However, evidence of extensive burrowing is also common within cycles at intracycle facies contacts (Figure 15B1, 2). Presence of these burrowed surfaces within cycle successions, presumably caused by episodic periods of local nondeposition, could make it difficult for true cycle tops to be identified in some successions. In most cases, however, burrow fills at cycle tops contain sediment fill of deeper water facies (derived from overlying transgressive deposits), whereas intracycle burrows are more commonly filled with sediment similar to the facies in which they are formed (Figure 15B2).

Although lateral changes in facies composition along timelines are expected, tracing of cycles along the Apache Canyon dip transect demonstrates that such facies changes may make cycle correlation problematic in noncontinuous outcrop exposures and in the subsurface (i.e., 1-D data). An example of this situation is illustrated in Figure 18, which shows changes in facies stacking along a dip transect through the highstand succession of L3.2. These changes illustrate that cycle definition, which depends on facies stacking patterns, may differ from one facies tract to another. In this example, three cycles (averaging 6–7 ft [2 m] in thickness) can be defined in proximal-ramp to inner-platform areas, whereas only one (22 ft [7 m] thick) can be recognized in the central ramp crest. These changes in facies stacking are likely the result of the dominating role of higher energy conditions in the ramp crest compared with more

landward areas of the platform. In any case, resultant facies successions pose real problems for correlation of cycles and timelines across the platform. Note that such problems seem to be unique to the highstand, where accommodation-driven facies contrasts (and contrasts in wave energy) are greater. In the TST of HFS 3.2, by contrast, facies stacking is much more regular and continuous across the same part of the platform (Figure 17). This regularity indicates that cycle correlation is likely to be much more straightforward in the TST than in the HST of carbonate-platform sequences.

CONCLUSIONS

Leonardian outcrops in the Sierra Diablo of west Texas provide a wealth of key observations on the facies composition and architecture of middle Permian carbonate platform successions and offers some caveats for the interpretation of cycle architecture in similar settings. Among these observations and caveats are the following:

- Platform top high frequency sequences (HFS) display systematic development of facies tracts both in terms of facies and platform position.
- Neither the architecture nor the boundaries of these HFS are typically definable from platform margin sequence relationships.
- Unlike cycles, which dominantly comprise asymmetrical, upward shallowing stacks of facies; HFS can display symmetrical, upward shallowing stacks, or upward deepening facies stacks.
- HFS boundaries can be difficult to define in 1-D stratigraphic sections and are best defined in dip-parallel 2D sections especially in proximity to the ramp (platform) crest.

These observations form a fundamental basis for defining and interpreting the cycle and sequence stratigraphy as well as the eustatic history and patterns of facies distribution in Leonardian and other transitional icehouse/greenhouse carbonate platform successions.

ACKNOWLEDGMENTS

This research was funded by the U.S. Department of Energy under contract no. DE-AC26-98BC15105 and by sponsors of the Reservoir Characterization Research Laboratory: Amoco, Aramco, ARCO, BP International, Exxon, Fina, Japan National Oil Corporation, Marathon, Meridian, Oxy, Pennzoil, Petroleum Development Oman, Phillips, Shell Western, Shell Canada, Texaco, Total, and UNOCAL. Many of the concepts presented here have developed in part from discussions between the senior author and Charlie Kerans. Bill Fitchen introduced us to the excellent outcrops in Apache Canyon. Field assistance was provided by Jubal Grubb, Greg Ramirez, Neil Tabor, Lance Christian, and Rebecca Jones. We are indebted to Mr. Nelson Puett, late owner of the Puett Ranch, and Ron Stasny, former owner of the Figure 2 Ranch, for permitting us access to these world-class exposures. Lana Dieterich provided editorial assistance. Illustrations were prepared by the Bureau of Economic Geology Media Department under the direction of Joel Lardon, Manager. Publication was authorized by the Director, Bureau of Economic Geology, The University of Texas at Austin.

LIST OF REFERENCES

Angiolini, L., 2003, Permian climatic and paleogeographic changes in northern Gondwana; the Khuff Formation of interior Oman: Palaeogeography, Palaeoclimatology, Palaeoecology, v. 191, p. 269-300.

Ariza, E. E., 1998, High resolution sequence stratigraphy of the Leonardian lower Clear Fork Group in the Permian Basin, West Texas: The University of Texas at Austin, Master's thesis, 128 p.

Atchley, S. C., Kozar, M. G., and Yose, L. A., 1999, A predictive model for reservoir characterization in the Permian (Leonardian) Clear Fork and Glorieta Formations, Robertson Field area, West Texas: AAPG Bulletin, v. 83, p. 1031-1056.

Ball, M. M., 1967, Carbonate sand bodies of Florida and the Bahamas: Journal of Sedimentary Petrology, v. 37, p. 556-591.

Barnaby, R. J., and Ward, W. B., 2007, Outcrop analog for mixed siliciclastic-carbonate ramp reservoirs; stratigraphic hierarchy, facies architecture, and geologic heterogeneity; Grayburg Formation, Permian Basin, U.S.A.: Journal of Sedimentary Research v. 77, p. 34-58

Beales, F. W., 1965, Diagenesis in pelleted limestones, *in* Pray, L. C., and Murray, R. C. (editors), Dolomitization and limestone diagenesis—a symposium: SEPM Special Publication No. 13, p. 49-70.

Bebout, D. G. Lucia, F. J., Hocott, C. R., Fogg, G. E., and Vander Stoep. G. W., 1987, Characterization of the Grayburg reservoir, University Lands Dune field, Crane County, Texas: Bureau of Economic Geology Report of Investigations 168, 98 p.

Dunham, R. J., 1961, Classification of carbonate rocks according to depositional texture, *in* Ham, W. E. (editor), Classification of carbonate rocks: AAPG Memoir 1, p. 108-121.

Fitchen, W. M., 1997, Lower Permian sequence stratigraphy of the western Delaware Basin margin, Sierra Diablo, West Texas: The University of Texas at Austin, Ph.D. dissertation, 264 p.

Fitchen, W. M., Starcher, M. A., Buffler, R. T., and Wilde, G. L., 1995, Sequence stratigraphic framework and facies models of the early Permian platform margins, Sierra Diablo, West Texas, *in* Garber, R. A., and Lindsay, R. F. (editors), Wolfcampian-Leonardian shelf margin facies of the Sierra Diablo—seismic scale models for subsurface exploration: West Texas Geological Society Publication No. 95-97, p. 23-66.

Hardie, L. A. and Shinn, E. A., 1986, Carbonate depositional environments, modern and ancient, Part 3: Tidal flats: Colorado School of Mines Quarterly, v. 81, no. 1, 74 p.

Harris, P. M., 1979, Anatomy and growth history of a Holocene ooid shoal: Sedimenta 7, 163 p.

Jennings, J. W., Jr., Ruppel, S. C., and Ward, W. B., 2000, Geostatistical analysis of permeability data and modeling of fluid-flow effects in carbonate outcrops: Society of Petroleum Engineers Reservoir Evaluation and Engineering, v. 3, no. 4, p. 292-303.

Kaufman, J., 1991, A predictive model for early dolomitization in the Permian Basin: Exxon Production Research, Unpublished Report EPR.6X.91, 31 p.

Kerans, C., and Fitchen, W. M., 1995, Sequence hierarchy and facies architecture of a carbonate ramp system: San Andres Formation of Algerita Escarpment and Western Guadalupe Mountains, West Texas and New Mexico: The University of Texas at Austin, Bureau of Economic Geology Report of Investigations No. 235, 86 p.

Kerans, C., and Kempter, K., 2002, Hierarchical stratigraphic analysis of a carbonate platform, Permian of the Guadalupe Mountains: The University of Texas at Austin, Bureau of Economic Geology (American Association of Petroleum Geologists/Datapages Discovery Series No. 5), CD-ROM.

Kerans, C., Kempter, K., Rush, J., and Fisher, W. L., 2000, Facies and stratigraphic controls on a coastal paleokarst: Lower Permian, Apache Canyon, West Texas, *in* R. Lindsay, Trentham, R., Ward, R. F., and Smith, A. H., (editors), Classic Permian geology of West Texas and Southeastern New Mexico, 75 Years of Permian Basin oil & gas exploration & development: West Texas Geological Society Publication No. 00-108, p. 55-82.

Kerans, C., Lucia, F. J., and Senger, R. K., 1994, Integrated characterization of carbonate ramp reservoirs using Permian San Andres Formation outcrop analogs: AAPG Bulletin, v. 78, no. 2, p. 181-216.

Kerans, C., and Ruppel, S. C., 1994, San Andres sequence framework, Guadalupe Mountains: implications for San Andres type section and subsurface reservoirs, *in* Garber, R. A., and Keller, D. R., eds., Field guide to the Paleozoic section of the San Andres Mountains: Permian Basin Section—SEPM (Society for Sedimentary Geology), Publication No. 94-35, p. 105–115.

King, P. B., 1942, Permian of West Texas and southeastern New Mexico: American Association of Petroleum Geologists Bulletin, v. 26, no. 4, p. 535-763.

King, P. B., 1965, Geology of the Sierra Diablo region, Texas: U.S. Geological Survey Professional Paper 480, 185 p.

Lucia, F. J., and Ruppel, S. C., 1996, Characterization of diagenetically altered carbonate reservoirs, South Cowden Grayburg reservoir, West Texas: Society of Petroleum Engineers, Paper SPE 36650, p. 883-893.

Mazzullo, S. J., 1982. Stratigraphy and depositional mosaics of lower Clear Fork and Wichita groups (Permian), northern Midland Basin, Texas: AAPG Bulletin 66, no. 2: 210-227.

Mazzullo, S. J., and A. Reid, 1989, Lower Permian platform and basin depositional systems, northern Midland Basin, Texas, *in* Crevello, P. D. Wilson, J., Sarg, J. F., and Read, J. F. (editors), Controls on carbonate platform and basin development: SEPM Special Publication, v. 44, p. 305-320.

Mertmann, D., 2003, Evolution of the marine Permian carbonate platform in the Salt Range (Pakistan): Palaeogeography, Palaeoclimatology, Palaeoecology, v. 191, p. 373-384.

Milliman, J. D., 1974, Marine carbonates: Springer-Verlag, New York, 375 p.

Montañez, I. P., and Osleger, D. A., 1993, Chapter 12. Parasequence stacking patterns, third-order accommodation events and sequence stratigraphy of Middle to Upper Cambrian platform carbonates, Bonanza King Formation, southern Great Basin,

in Loucks, R. G., and Sarg, F. R. (editors), Carbonate sequence stratigraphy: recent developments and applications: AAPG Memoir 57, p. 305-326.

Montañez, I. P., Tabor, N. J., Niemeier, D., DiMichele, W. A., Frank, T. D., Fielding, C. R., Isbell, J. L., Birgenheier, L. P., and Ryge, M. C., 2007, CO_2-forced climate and vegetation instability during late Paleozoic deglaciation: Science v. 315, no. 5808, p. 87-91.

Multer, H. G., 1977, Field guide to some carbonate rock environments Florida Keys and western Bahamas: Kendall/Hunt, Dubuque, Iowa, 415 p.

Osleger, D. A., and Montanez, I. P., 1996, Cross-platform architecture of a sequence boundary in mixed siliciclastic-carbonate lithofacies, Middle Cambrian, southern Great Basin, USA: Sedimentology, v. 43, no. 2, p. 197-217.

Osleger, D. A., and Read, J. F., 1991, Relation of eustasy to stacking patterns of meter-scale carbonate cycles, Late Cambrian, USA: Journal of Sedimentary Petrology, V 61, p. 1225-1252.

Purdy, E. G., 1963, recent calcium carbonate facies of the great Bahama Bank, 2: sedimentary facies: Journal of Geology v. 71, p. 472-497.

Read, J. F., 1995, Part 1. Overview of carbonate platform sequences, cycle stratigraphy and reservoirs in greenhouse and icehouse worlds, *in* Read, J. F., Kerans, C., Weber, L. J., Sarg, J. F., and Wright, F. M. (editors), Milankovitch sea-level changes, cycles, and reservoirs on carbonate platforms in greenhouse and icehouse worlds: SEPM Short Course 35, p. 1-102.

Ross, C. A., and Ross, J. R. P., 2003, Sequence evolution and sequence extinction; fusulinid biostratigraphy and species-level recognition of depositional sequence, Lower Permian, Glass Mountains, West Texas, U.S.A., *in* Olson, H. C., and Leckie, R. M. (editors), Micropaleontologic proxies for sea-level change and stratigraphic discontinuities: (SEPM) Society for Sedimentary Geology Special Publication 75, p. 317-359.

Ruppel, S. C., 1992, Styles of deposition and diagenesis in Leonardian carbonate reservoirs in West Texas: implications for improved reservoir characterization: Society of Petroleum Engineers Annual Exhibition and Technical Conference, 24691, p. 313-320.

Ruppel, S. C., 2002, Geological controls on Leonardian reservoir development, Monahans Clear Fork field, West Texas: The University of Texas at Austin, Bureau of Economic Geology Report of Investigations No. 266, 58 p.

Ruppel, S. C., and Bebout, D. G., 2001, Competing effects of depositional architecture and diagenesis on carbonate reservoir development: Grayburg Formation, South Cowden field, West Texas: The University of Texas at Austin, Bureau of Economic Geology Report of Investigations No. 263, 62 p.

Ruppel, S. C., and Cander, H. S., 1988a, Effects of facies and diagenesis on reservoir heterogeneity: Emma San Andres field, West Texas: The University of Texas at Austin, Bureau of Economic Geology Report of Investigations No. 178, 67 p.

Ruppel, S. C., and Cander, H. S., 1988b, Dolomitization of shallow-water platform carbonates by sea water and seawater-derived brines: San Andres Formation (Guadalupian), West Texas, *in* Sedimentology and geochemistry of dolostones: Society of Economic Paleontologists and Mineralogists, Special Publication No. 43, p. 245-262.

Ruppel, S. C., and Jones, R. H., 2007, Chapter 10. Key role of outcrops and cores in carbonate reservoir characterization and modeling, Lower Permian Fullerton field, Permian Basin, United States, *in* Harris, P. M., and Weber, L. J. (editors), Giant hydrocarbon reservoirs of the world: from rocks to reservoir characterization and modeling: AAPG Memoir 88/SEPM Special Publication, p. 355-394.

Ruppel, S. C. , Kerans, C., Major, R. P., and Holtz, M. H., 1995, Controls on reservoir heterogeneity in Permian Basin shallow-water platform carbonate reservoirs, Permian Basin: implications for secondary recovery: The University of Texas at Austin, Bureau of Economic Geology Geological Circular 95-2, 30 p.

Ruppel, S. C., W. B. Ward, E. E. Ariza, and J. W. Jennings, Jr., 2000, Cycle and sequence stratigraphy of Clear Fork reservoir-equivalent outcrops: Victorio Peak Formation, Sierra Diablo, Texas, in R. Lindsay, R. Trentham, R. F. Ward, and A. H. Smith, eds., Classic Permian geology of West Texas and Southeastern New Mexico, 75 years of Permian Basin oil & gas exploration & development: West Texas Geological Society Publication 00-108, p. 109–130.

Saller, A. H., and Henderson, N., 1998, Distribution of porosity and permeability in platform dolomites: insights from the Permian of west Texas: AAPG Bulletin, v. 82, no. 8, p. 1528-1550.

Sharland, P. R., Archer, R., Casey, D. M., Davies, R. B., Hall, S. H., Heward, A. P., Horbury, A. D., and Simmons, M.D., 2001, Arabian plate sequence stratigraphy: GeoArabia Special Publication 2, Gulf PetroLink, Bahrain, 371 p.

Shinn, E. A., 1983, Chapter 4. Tidal flat, *in* Scholle, P. A., Bebout, D. G., and Moore, C. H. (editors), Carbonate depositional environments: AAPG Memoir 33, p. 171-210.

Shinn, E. A. and Robbin, D. M., 1983, Mechanical and chemical compaction in fine-grained shallow-water limestones: Journal of Sedimentary Petrology, v. 53, no. 2, p. 595-618

Sonnenfeld, M. D., 1991, High-frequency cyclicity within shelf-margin and slope strata of the upper San Andres sequence, Last Chance Canyon, *in* Meader-Roberts, Sally, Candelaria, M. P., and Moore, G. E. (editors), Sequence stratigraphy, facies and reservoir geometries of the San Andres, Grayburg, and Queen Formations, Guadalupe Mountains, New Mexico and Texas: Permian Basin Section, Society of Economic Paleontologists and Mineralogists Publication 91-32, p. 11–51.

Stemmerik, L., 2001, Sequence stratigraphy of a low productivity carbonate platform succession; the Upper Permian Wegener Halvo Formation, Karstryggen area, East Greenland: Sedimenology v. 48, p. 79-97.

Strohmenger, C. and Strauss, C., 1996, Sedimentology and palynofacies of the Zechstein 2 carbonate (Upper Permian, Northwest Germany); implications for sequence stratigraphic subdivision: Sedimentary Geology v. 102, p. 55-77.

Strohmenger, C., Voight, E., and Zimdars, J, 1996, Sequence stratigraphy and cyclic development of Basal Zechstein carbonate-evaporite deposits with emphasis on Zechstein 2 off-platform carbonates (Upper Permian, Northeast Germany): Sedimentary Geology v. 102, p. 33-54.

Tucker M. E., 1991, Sequence stratigraphy of carbonate-evaporite basins; models and application to the Upper Permian (Zechstein) of Northeast England and adjoining North Sea. Journal of the Geological Society of London 148, p. 1019-1036.

Tyler, Noel, and Banta, N. J., 1989, Oil and gas resources remaining in the Permian Basin: targets for additional hydrocarbon recovery: The University of Texas at Austin, Bureau of Economic Geology Geological Circular 89-4, 20 p.

Veevers, J. J., and Powell, C. M. 1987. Late Paleozoic glacial episodes in Gondwanaland reflected in transgressive-regressive depositional sequences in Euramerica: Geological Society of America Bulletin: v. 98, p. 475-487.

Ye, Q., and Mazzullo, S.J., 1993, Dolomitization of Lower Permian platform facies, Wichita Formation, North Platform, Midland Basin, Texas: Carbonates and Evaporites , v. 8, p. 55-70

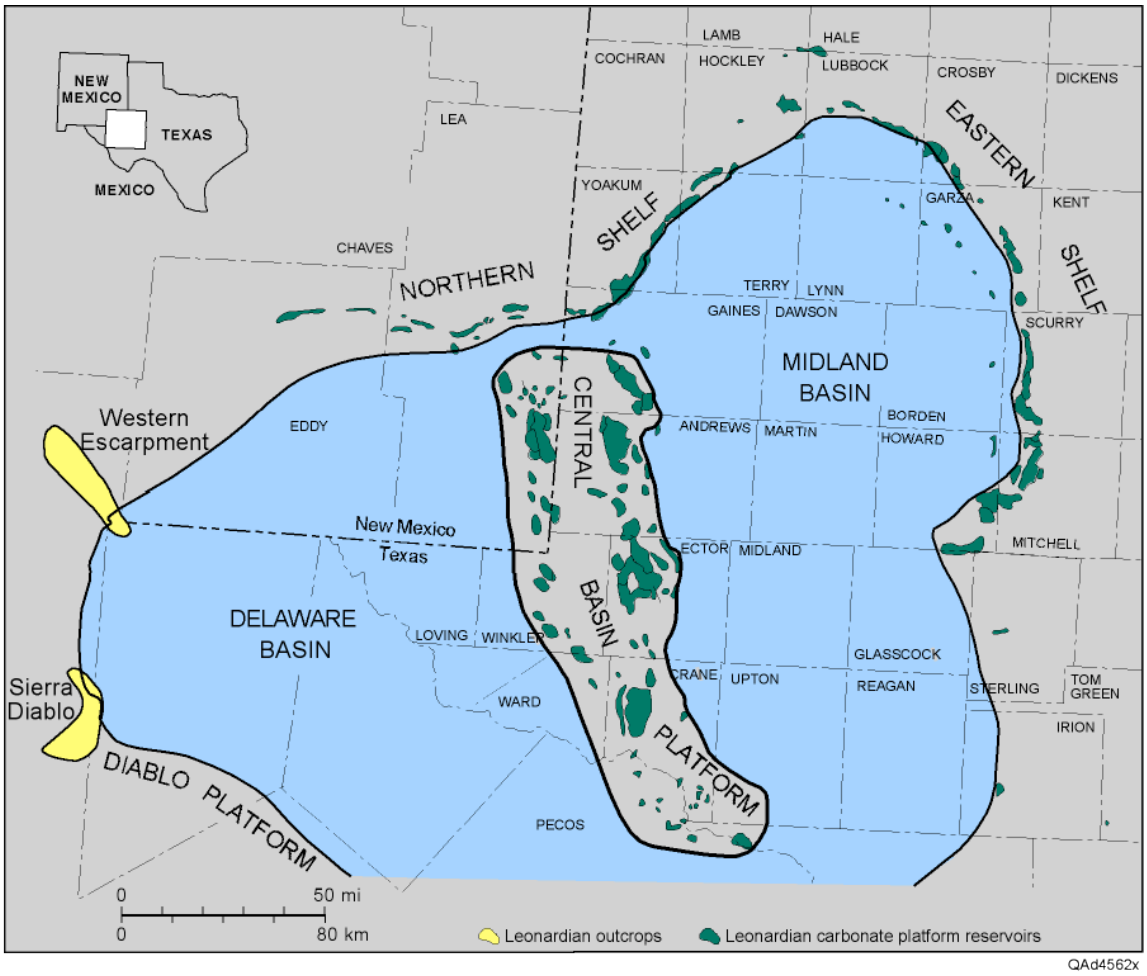

Figure 1. Paleogeographic map of the west Texas and southeastern New Mexico area during the early-middle Permian showing locations of major outcrops and subsurface reservoirs in the Permian Basin.

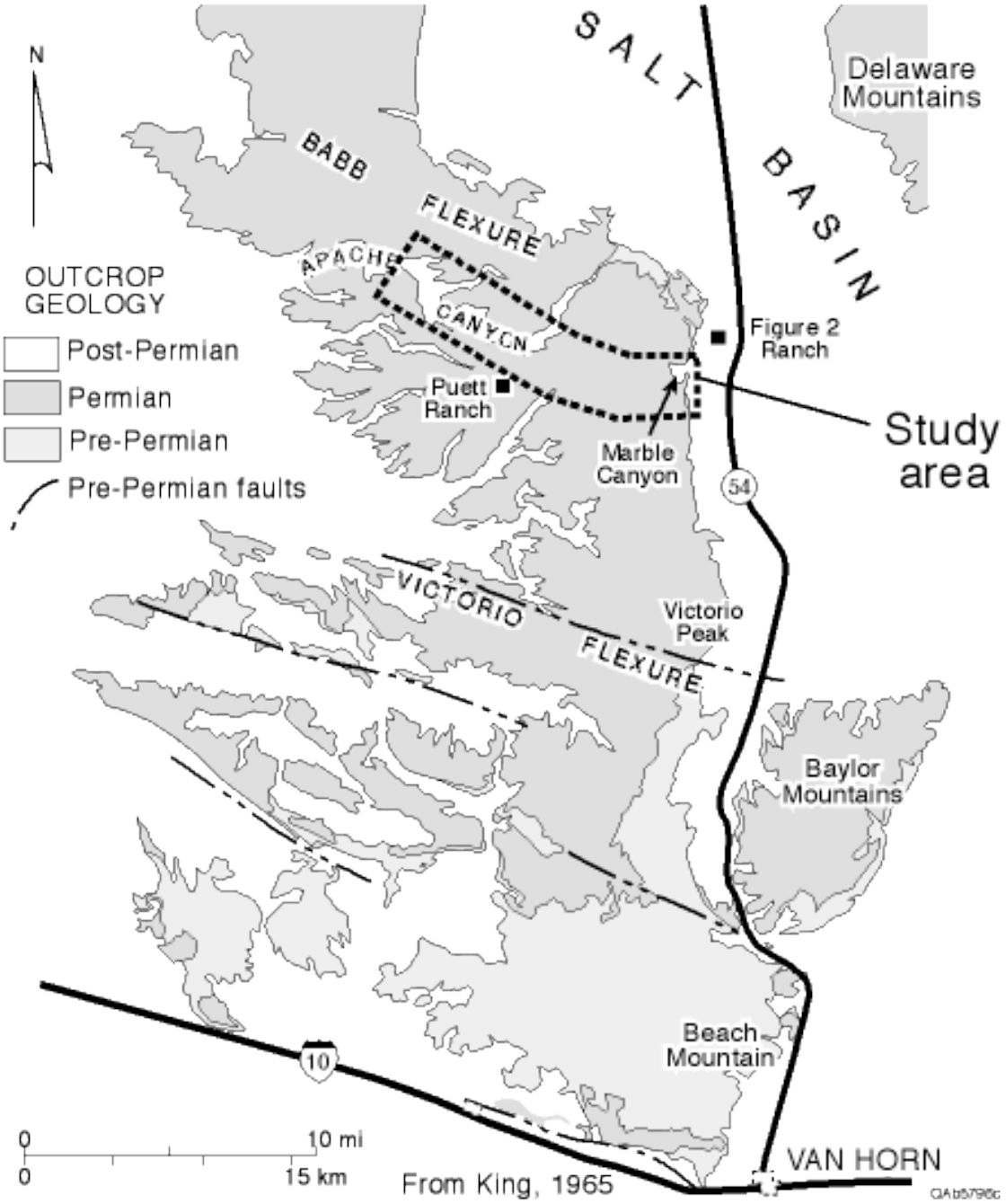

Figure 2. Map of Sierra Diablo area showing geology and location of study area.

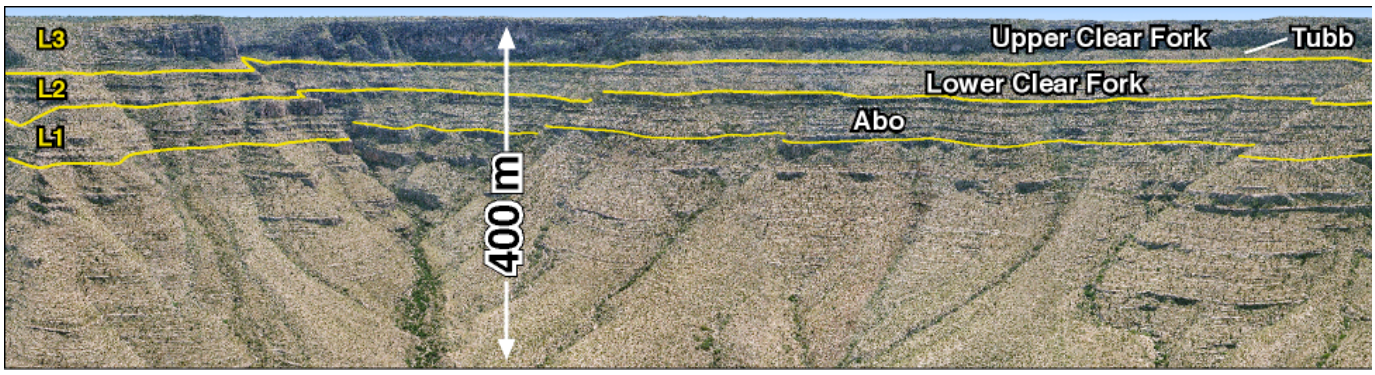

Figure 3. Photomosaic of south wall of Apache Canyon showing major sequence and formation boundaries. Distance along the rim is about 2 mi (3 km).

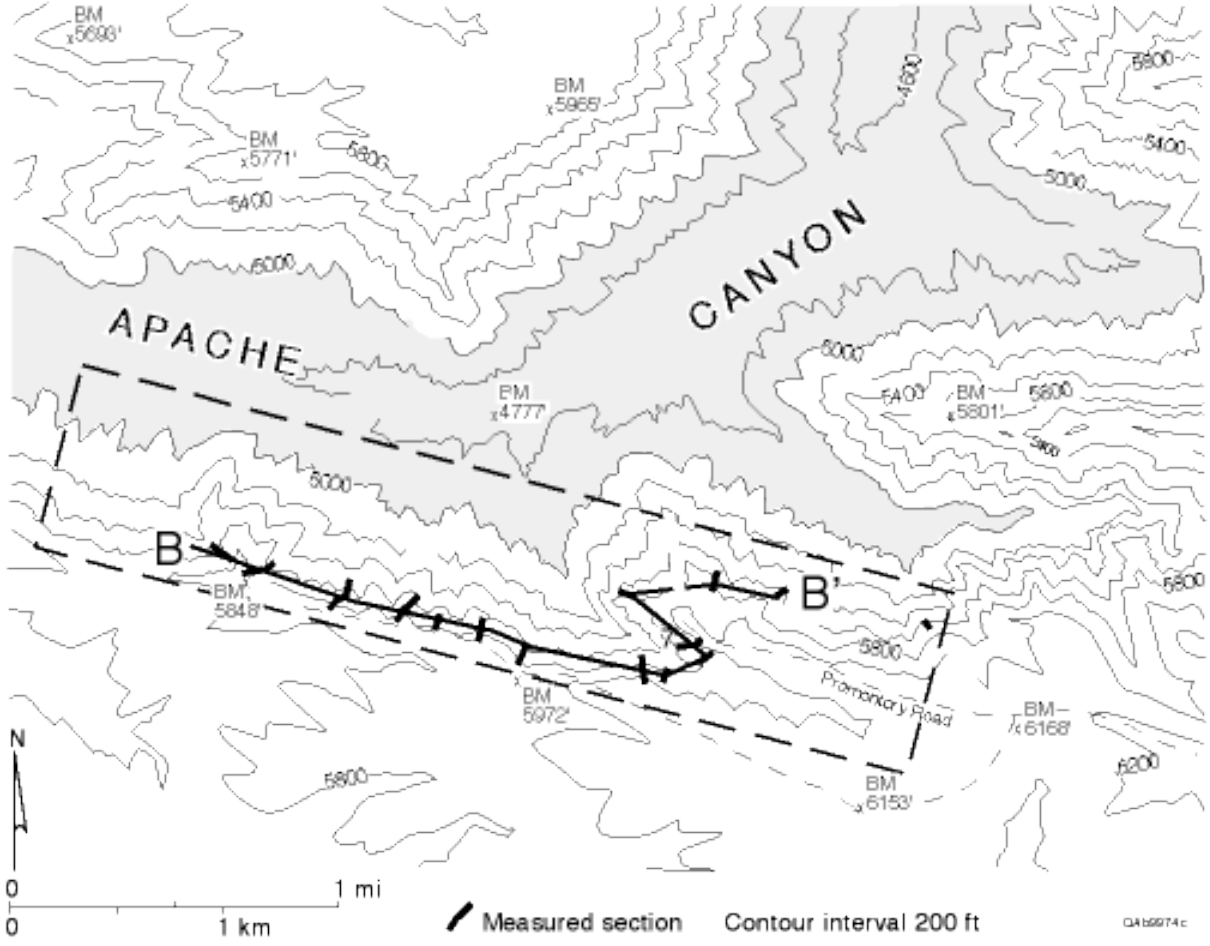

Figure 4. Topographic map of part of Apache Canyon showing the location of the study area and line of section shown in Figure 12.

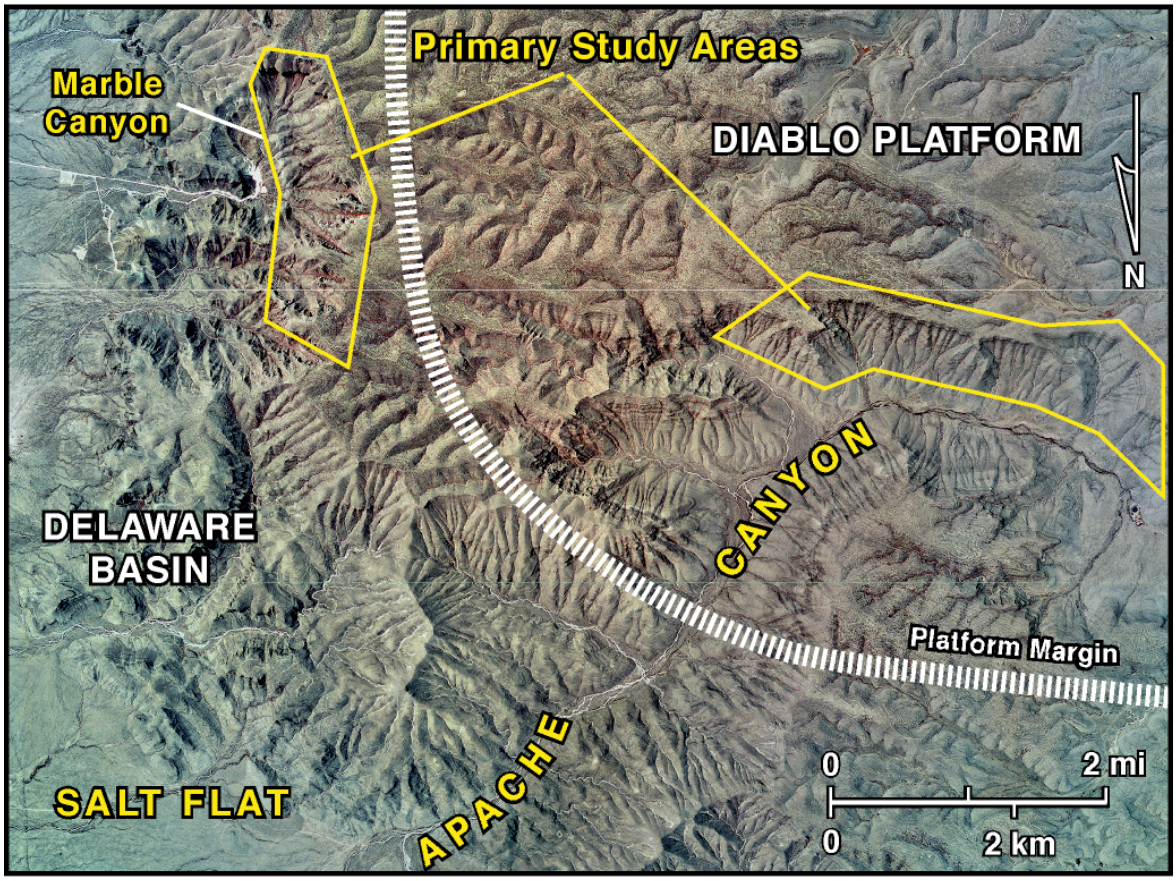

Figure 5. High-altitude, false-color infrared photography of region showing primary study area in Apache Canyon and secondary study area in Marble Canyon.

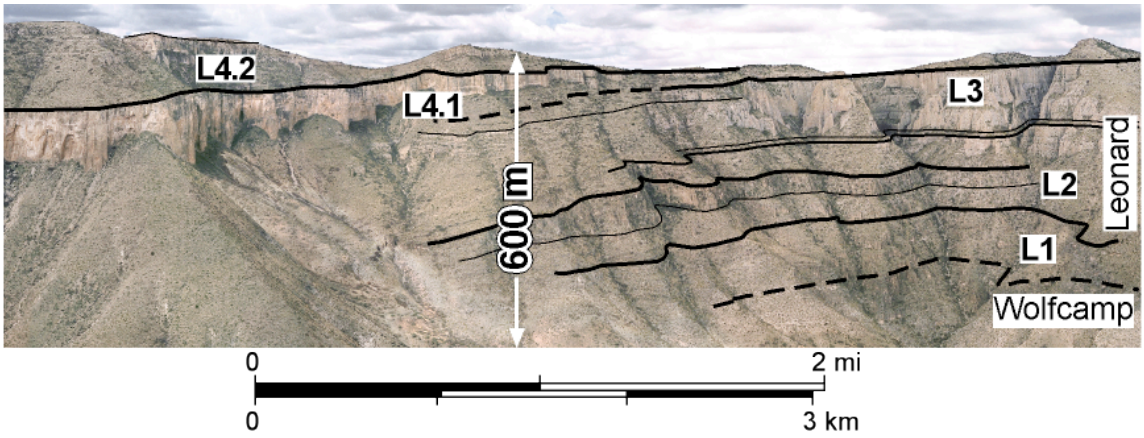

Figure 6. Outcrop photomosaic showing platform-margin expression of Leonardian facies in Marble Canyon. Resistant ledges comprise clinoformal successions of fusulinid-crinoid packstones and wackestones, whereas poorly exposed, intervening intervals are composed of sparsely fossiliferous, cherty mudstones assigned to the Bone Spring Formation Sequences 1–3 comprise thick, basinward-stepping, clinoformal successions of outer-platform to slope fusulinid-crinoid packstones and wackestones overlying Bone Spring mudstones. Note the well-defined, basinward-stepping wedges of sequence L4. Compare with Figure 10.

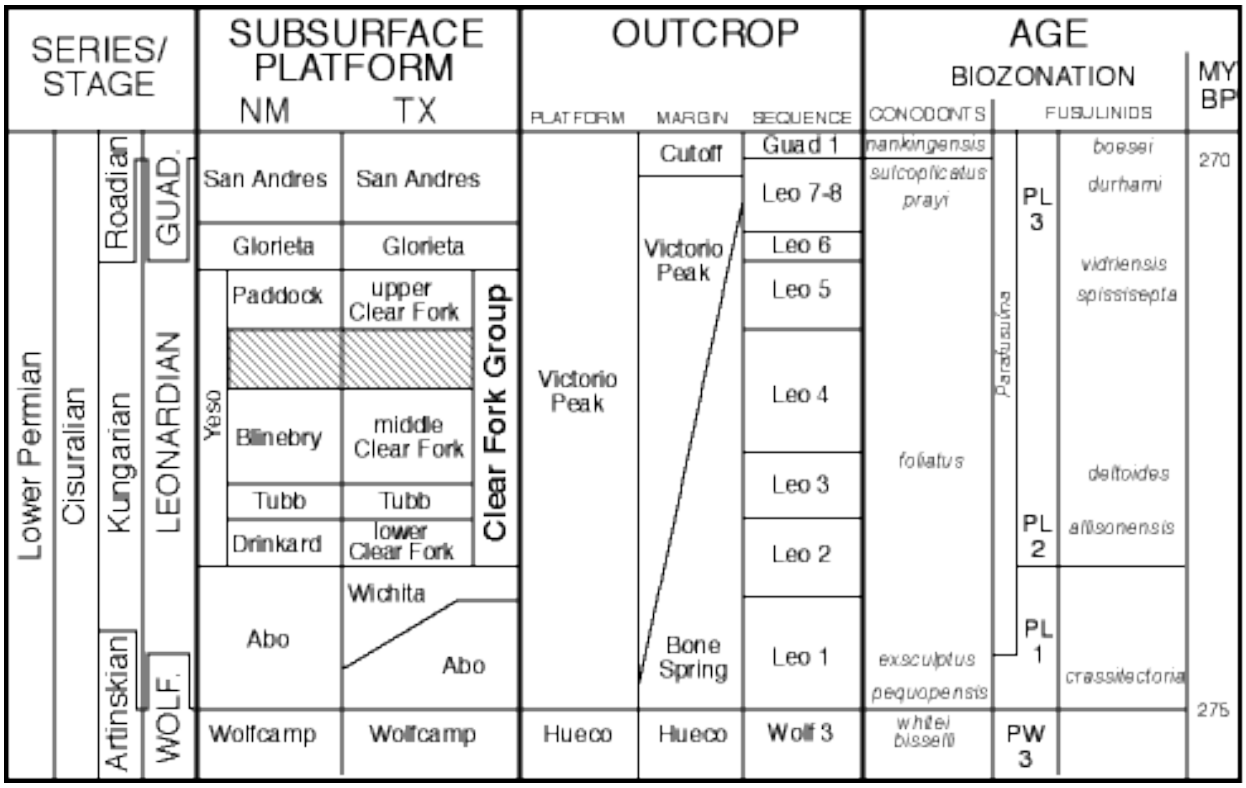

Figure 7. Stratigraphic nomenclature of Leonardian units in outcrop and subsurface areas of the Permian Basin region.

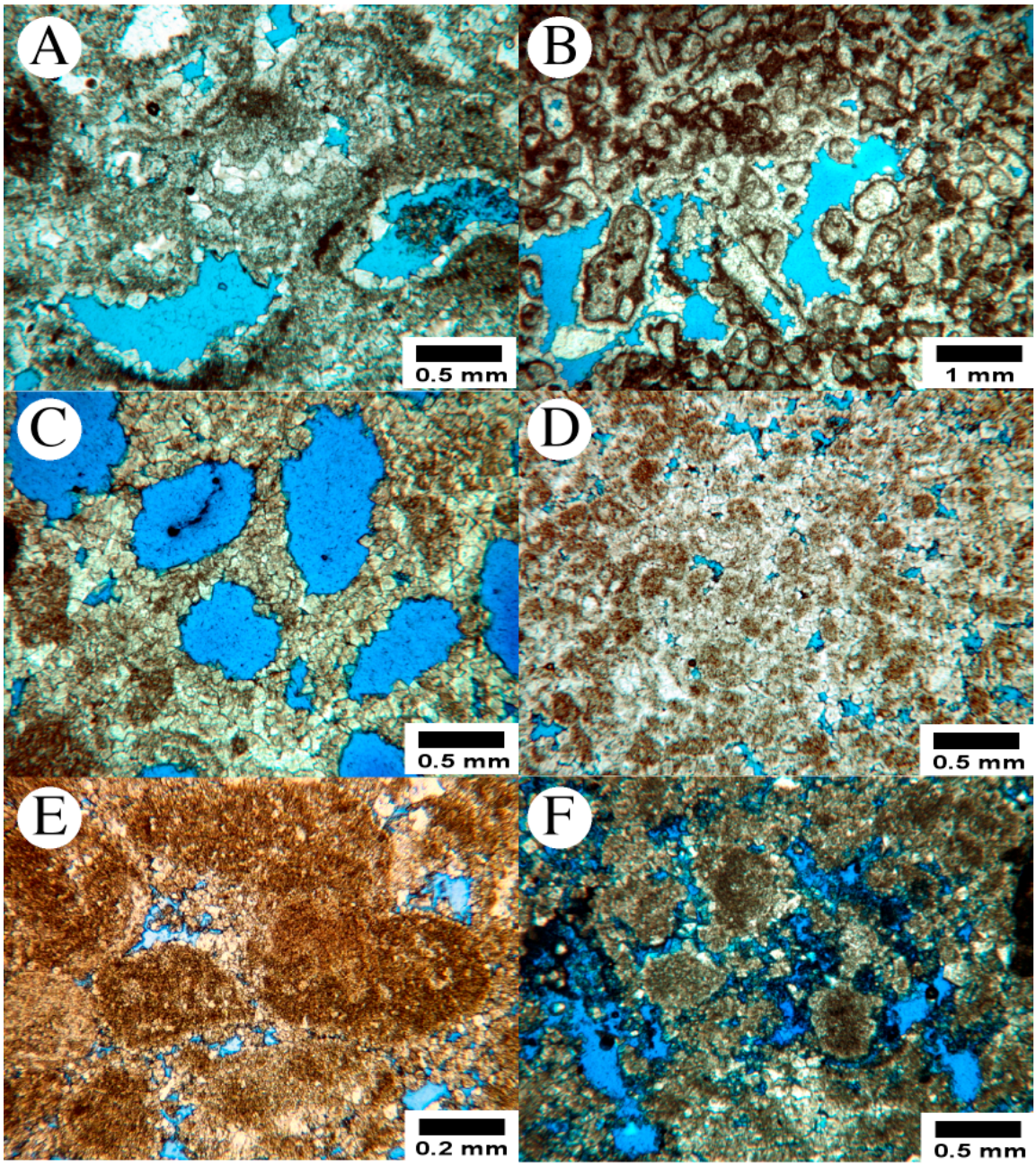

Figure 8. Thin-section photomicrographs of representative Clear Fork facies. A. Fenestral tidal-flat wackestone, HFS 2.1. B. Fenestral coated-grain packstone. HFS L.3.3 TST tidal flat. C. Fusulinid wackestone. HFS L.3.3 TST outer platform. D. Peloid grain-dominated packstone. HFS L.3.3 TST. E. Ooid/peloid grainstone. HFS L.3.3 TST. F. Ooid grainstone. HFS L.3.3 HST ramp crest.

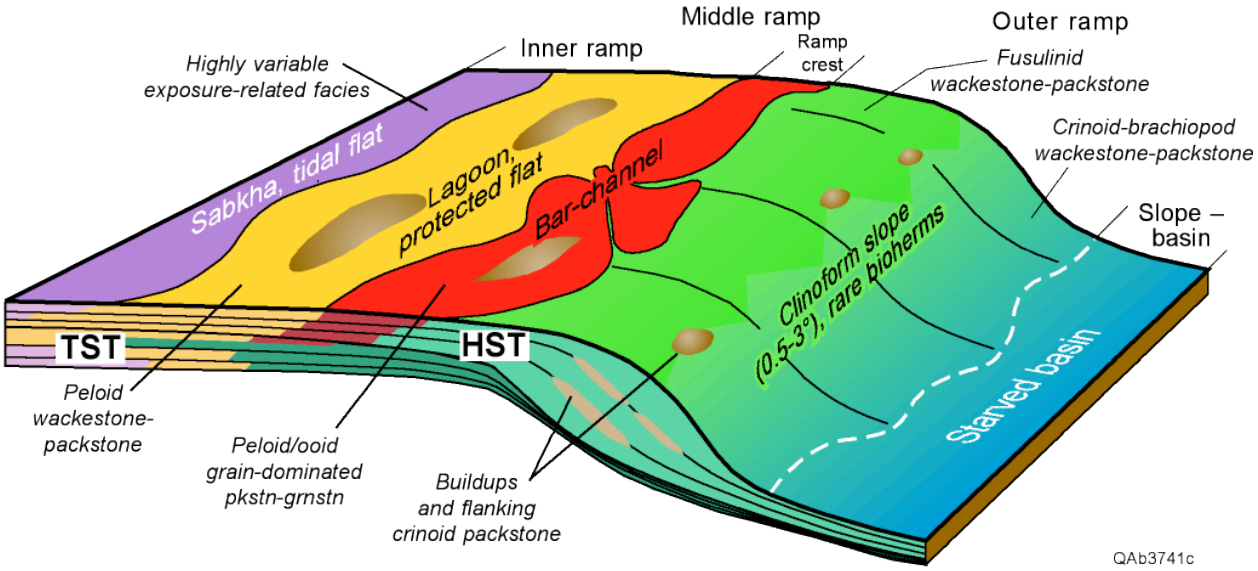

Figure 9. Depositional model for middle Permian, shallow-water carbonate platforms in the Permian Basin. From Ruppel and others (1995).

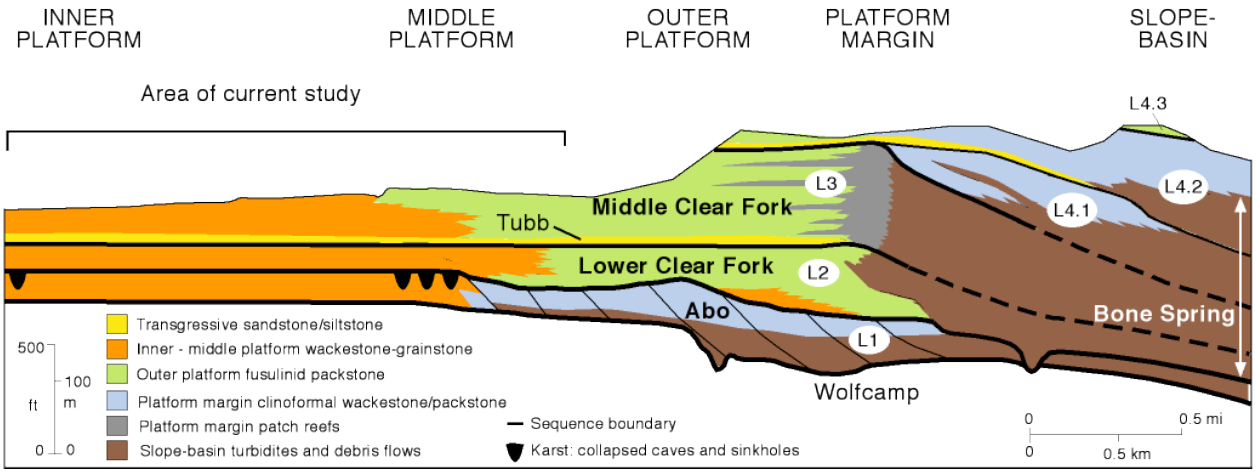

Figure. 10. Large-scale, sequence stratigraphic relationships in the Leonardian in Apache Canyon along approximate depositional dip. Modified from Fitchen and others (1995) and Kerans (2002).

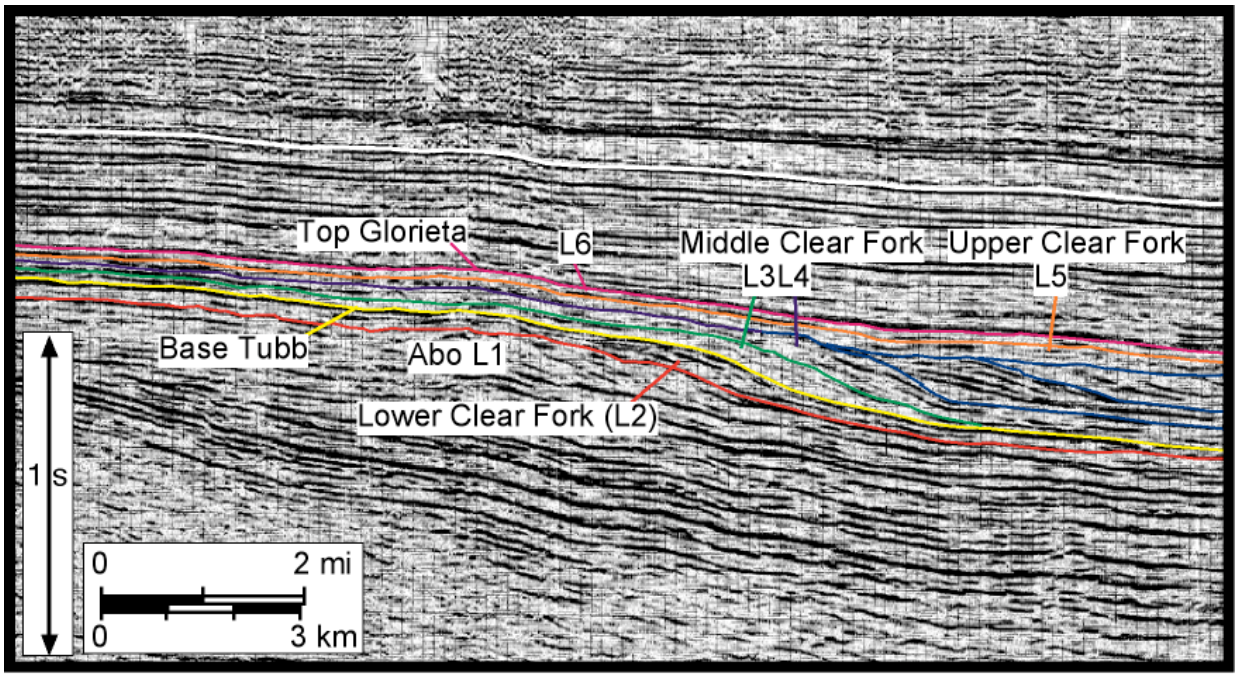

Figure 11. East-west 3-D seismic section showing typical expression of Leonardian sequence architecture in the subsurface of the Permian Basin. Most striking is the marked basinward progradation during the L4 expressed by eastward-stepping wedges. Compare with the outcrop expressions of sequence L4 in Figures 6 and 10.

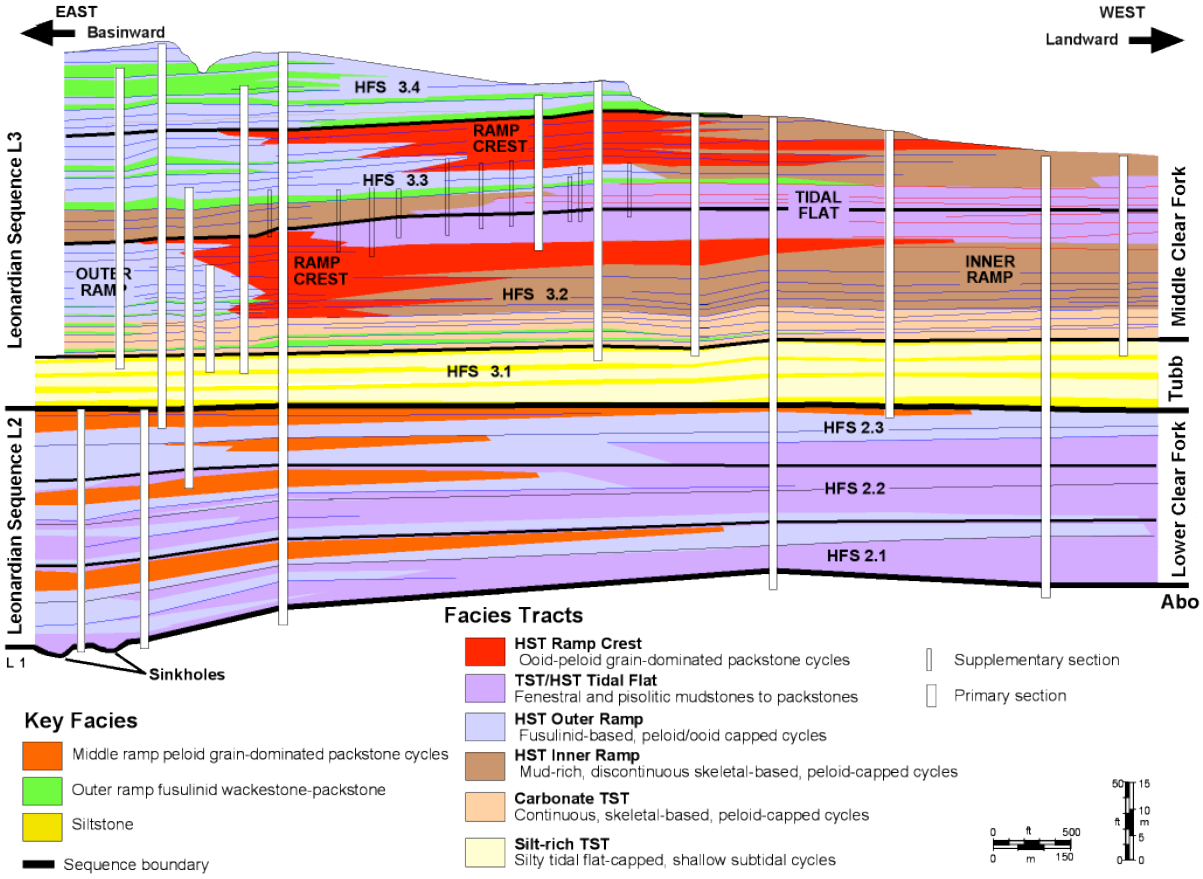

Figure 12. East-west cross section A-A′ along south wall of Apache Canyon showing architecture of facies tracts and high-frequency sequences in the Leonardian. Line of section shown in Figure 4.

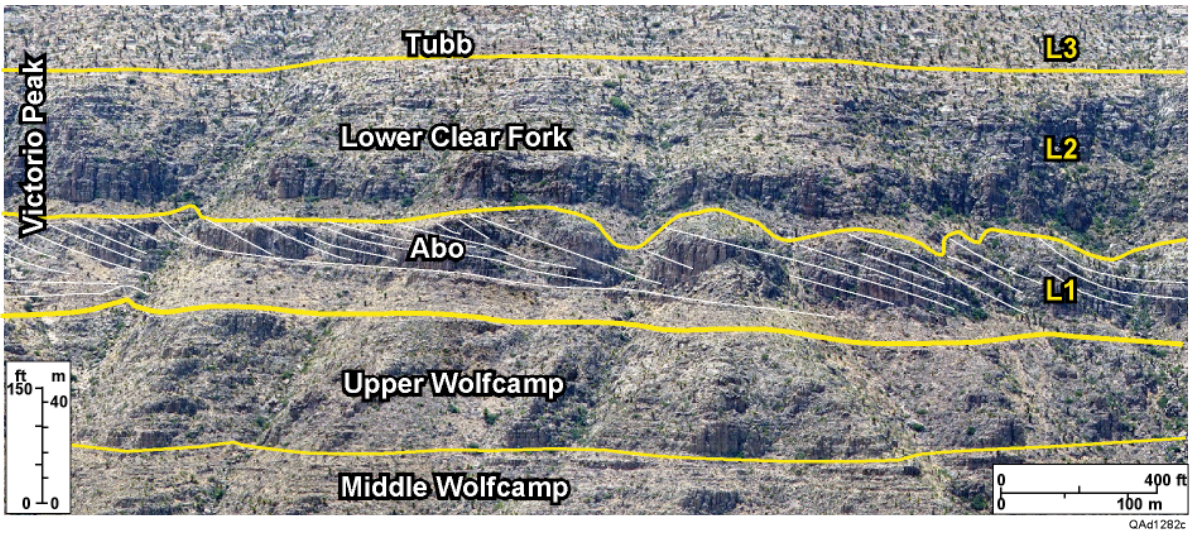

Figure 13. Outcrop photograph showing karst-related collapse topography at base of L2 sequence. Note top-lapping beds of L1 Abo outer-ramp facies and overlying basal L2 tidal-flat facies of the L2 Clear Fork infilling karst topography. See Kerans and others (2000) for details.

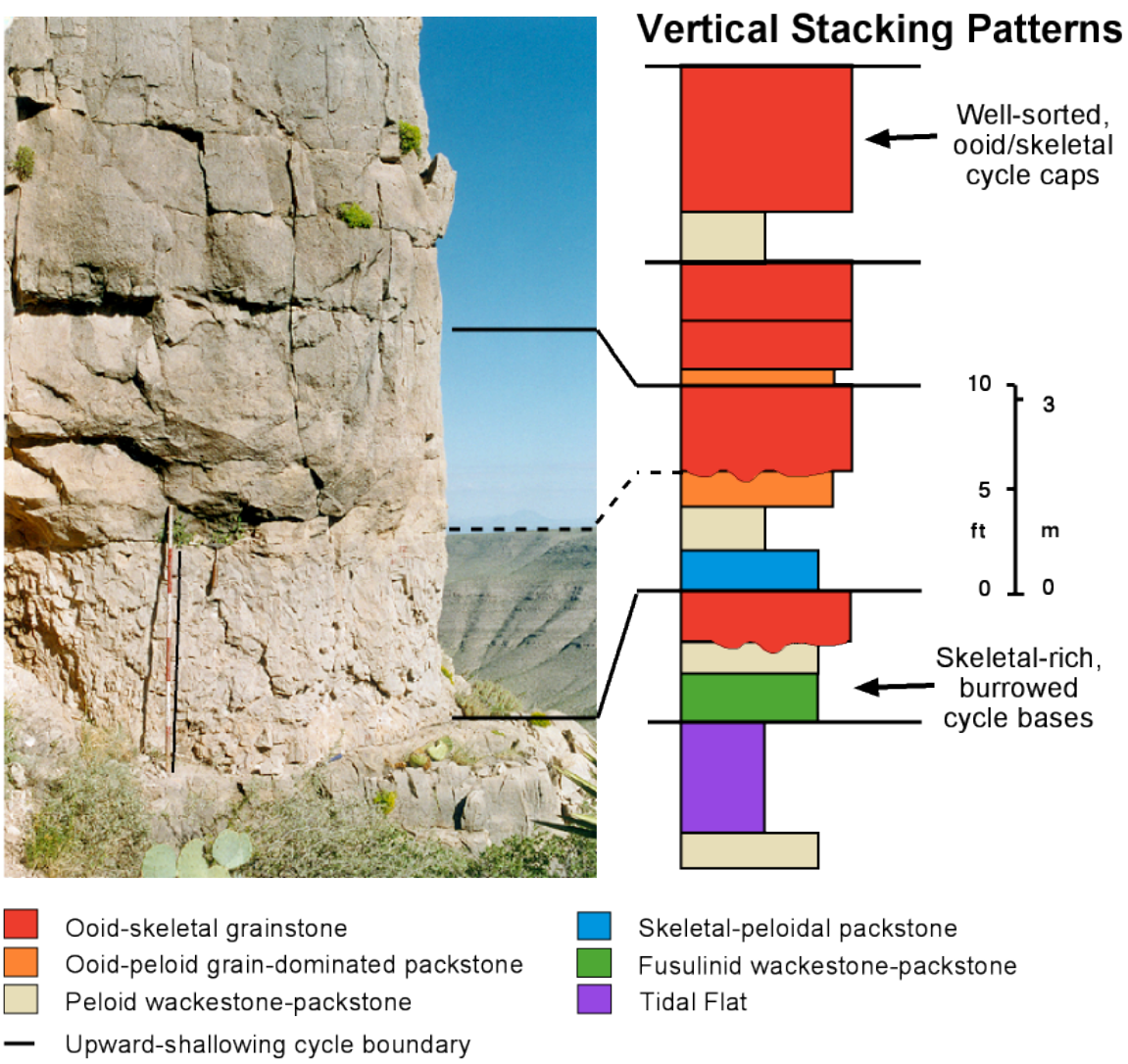

Figure 14. Outcrop photograph of typical high-accommodation transgressive cycle. Cycle base is composed of burrowed, fusulinid-rich wackestone; top is peloid-ooid packstone-grainstone. Staff rests on cycle base. HFS 3.3.

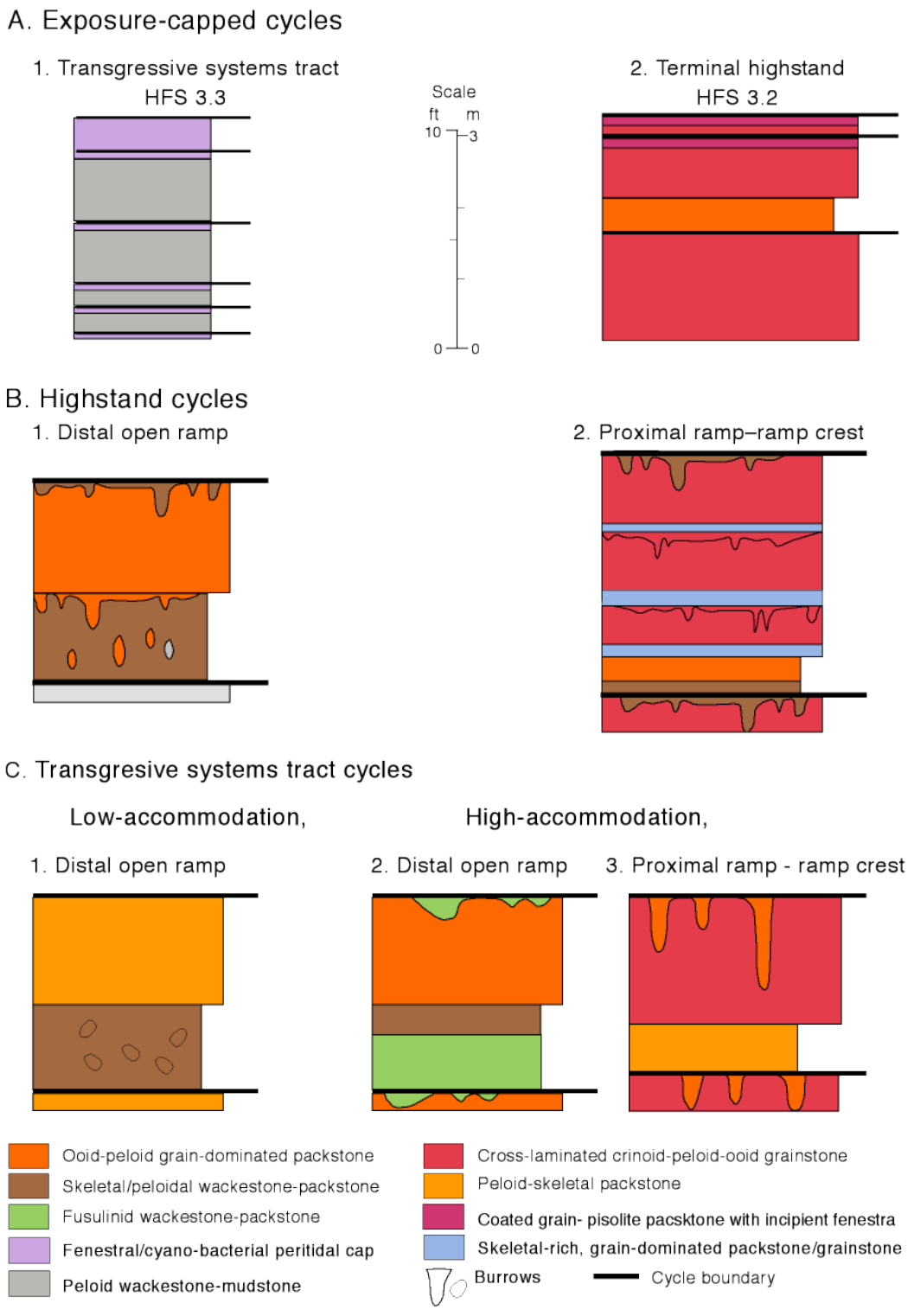

Figure 15. Styles of facies stacking in Leonardian platform systems tracts. A. High-accommodation transgressive systems tract cycles. B. Low-accommodation transgressive systems tract cycles. HFS 3.2. C. Exposure-capped cycles. D. Highstand systems tracts.

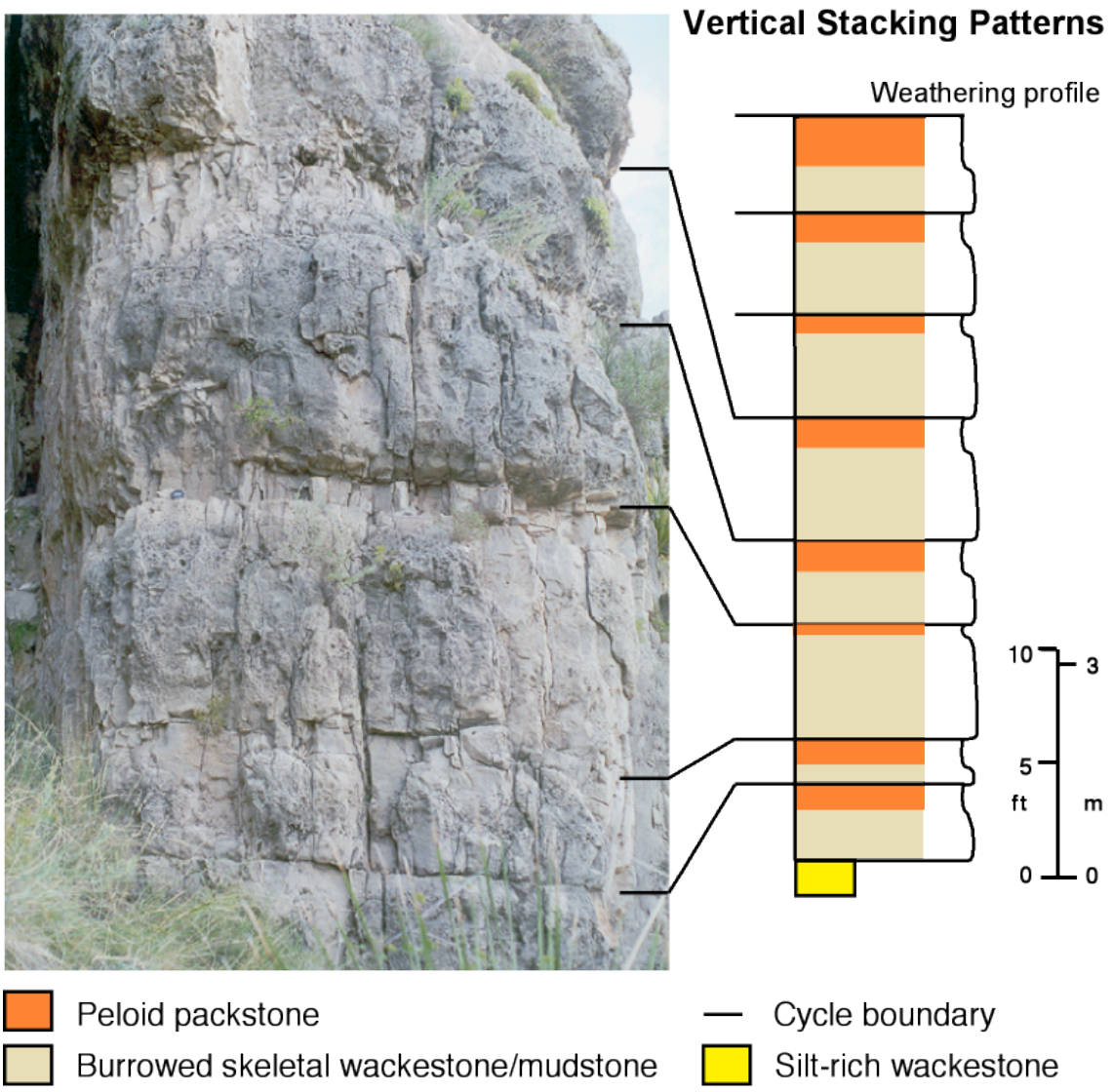

Figure 16. Outcrop expression of cyclicity in low-accommodation transgressive systems tract cycles. HFS 3.2.

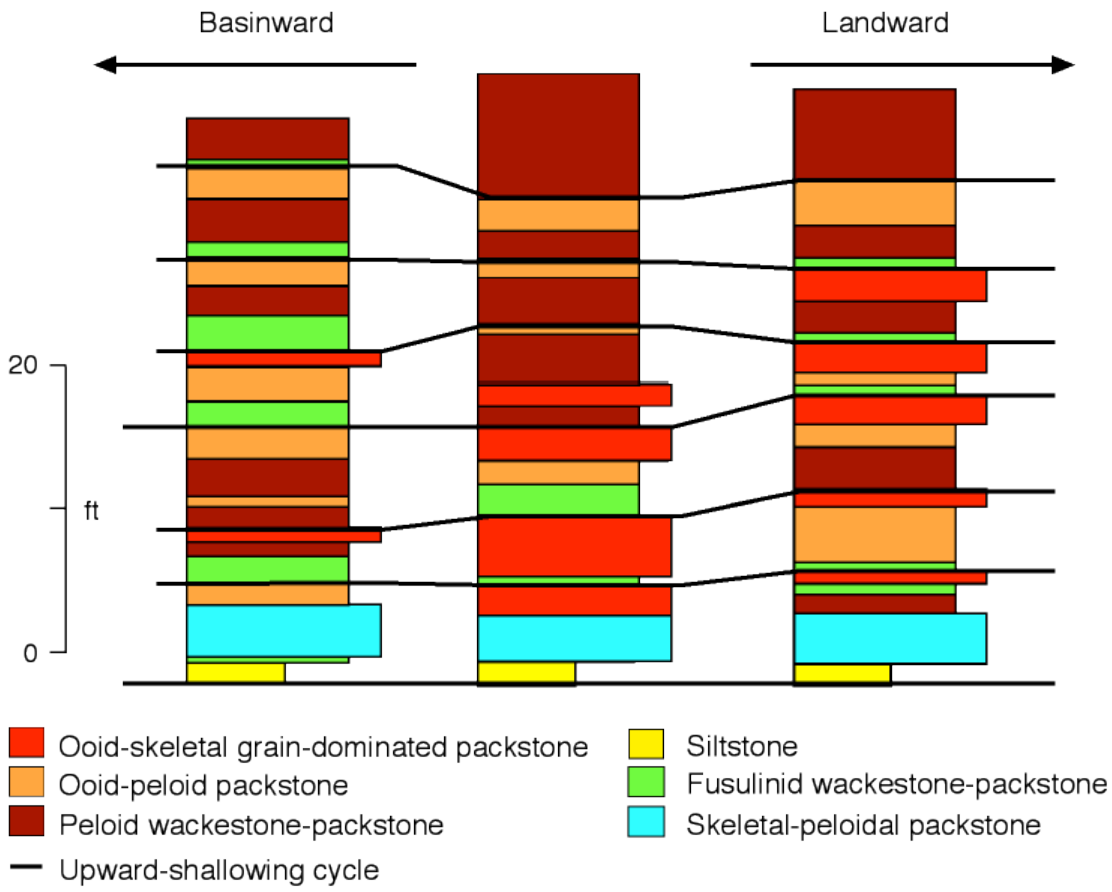

Figure 17. Lateral continuity of highly continuous transgressive cycles in HFS 3.1.

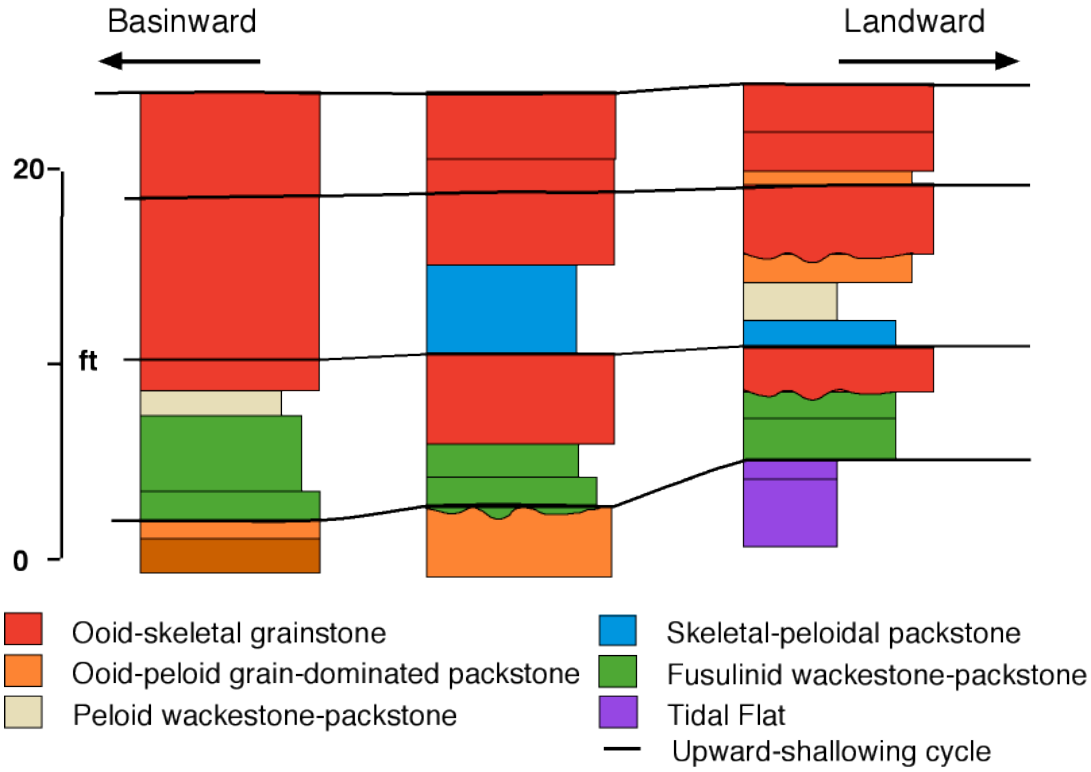

Figure 18. Lateral continuity of late transgressive cycles and early highstand cycles in the ramp-crest to inner-ramp area (HFS 3.2).